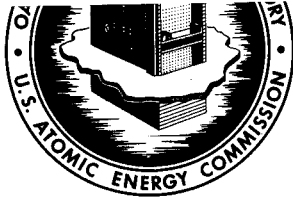




3 4456 0514421 5



OAK RIDGE NATIONAL LABORATORY

operated by

UNION CARBIDE CORPORATION • NUCLEAR DIVISION

for the

U. S. ATOMIC ENERGY COMMISSION



ORNL - TM - 3520

cy. 1

PHASE REPORT NO. 115-10

ON

COMPARISONS OF TEST DATA WITH CODE METHODS
FOR FATIGUE EVALUATION

E. C. Rodabaugh and S. E. Moore

NOTICE This document contains information of a preliminary nature and was prepared primarily for internal use at the Oak Ridge National Laboratory. It is subject to revision or correction and therefore does not represent a final report.

This report was prepared as an account of work sponsored by the United States Government. Neither the United States nor the United States Atomic Energy Commission, nor any of their employees, nor any of their contractors, subcontractors, or their employees, makes any warranty, express or implied, or assumes any legal liability or responsibility for the accuracy, completeness or usefulness of any information, apparatus, product or process disclosed, or represents that its use would not infringe privately owned rights.

Contract No. W-7405-eng-26

Reactor Division

PHASE REPORT NO. 115-10

on

COMPARISONS OF TEST DATA WITH CODE METHODS
FOR FATIGUE EVALUATION

E. C. Rodabaugh
Battelle Memorial Institute

S. E. Moore
Oak Ridge National Laboratory

NOVEMBER 1971

Subcontract No. 2913

for

OAK RIDGE NATIONAL LABORATORY
Oak Ridge, Tennessee 37830
operated by
UNION CARBIDE CORPORATION
for the
U.S. ATOMIC ENERGY COMMISSION



•

•

•

•

•

•

TABLE OF CONTENTS

	<u>Page</u>
FOREWORD	v
ABSTRACT	vi
NOMENCLATURE	vii
LIST OF TABLES	x
INTRODUCTION	1
EVALUATION PROCEDURE	3
MOMENT LOADING	7
Girth Butt Welds	9
Short Radius and Long Radius Elbows	13
Forged Welding Tees	17
Fabricated and Drawn Outlet Tees	19
Girth Fillet Welds	22
Notched Pipe	24
PRESSURE LOADING	29
Nozzles in Pressure Vessels-I	29
Nozzles in Pressure Vessels-II	33
Longitudinal Butt Welds in Pressure Vessels	36
THERMAL GRADIENT LOADING	40
COMPARISONS WITH ANSI B31.1 (POWER PIPING) FATIGUE DESIGN BASIS	47
Carbon Steel at Room Temperature	47
Carbon Steel at Elevated Temperatures	52
Austenitic Stainless Steel at Room Temperature	53
Austenitic Stainless Steel at Elevated Temperatures	55
Permissible Design Cycles	58
SUMMARY	62
REFERENCES	64
APPENDIX A - ASME BOILER CODE CASE 1441 AND POSSIBLE REVISIONS THEREOF	67



FOREWORD

The work reported here was done at Battelle Memorial Institute under Union Carbide Corp. Nuclear Division subcontract No. 2913, and with the assistance of Oak Ridge National Laboratory personnel as part of the ORNL Piping Program - Design Criteria for Piping, Pumps, and Valves. This program is being carried out for the U.S. Atomic Energy Commission by the Oak Ridge National Laboratory under the direction of W. L. Greenstreet, Associate Head, Solid Mechanics Department; and S. E. Moore, Program Coordinator. J. L. Mershon of the AEC Division of Reactor Development and Technology is the USAEC cognizant engineer.

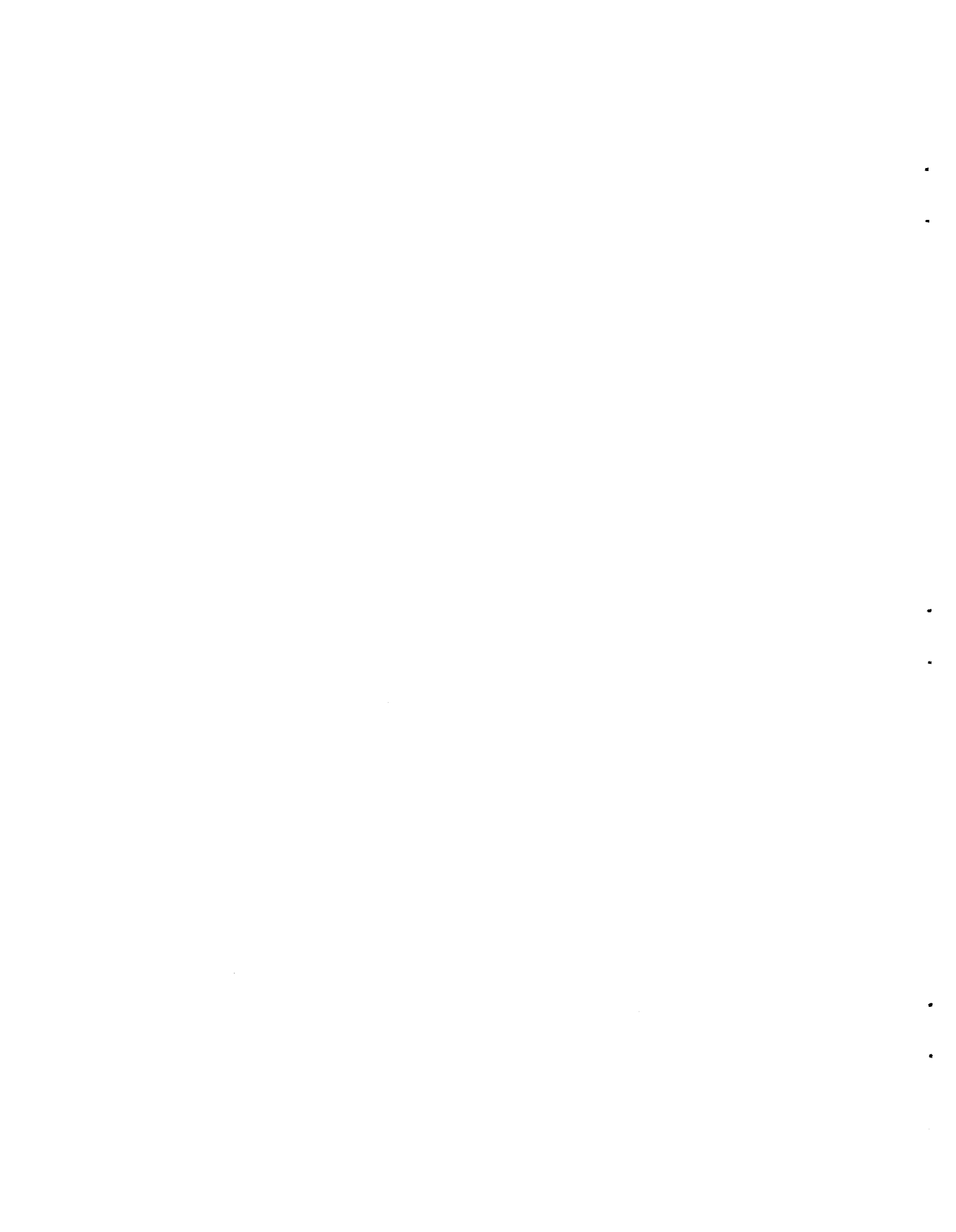
The ORNL Piping Program is funded by the USAEC under the Nuclear Safety Research and Development Program as the AEC supported portion of an AEC-Industry cooperative effort for the development of design criteria for nuclear power plant piping components, pumps, and valves. The AEC-Industry cooperative effort is coordinated by the Pressure Vessel Research Committee (PVRC) of the Welding Research Council.



ABSTRACT

In an effort to evaluate proposed design rules for the fatigue analysis of piping system components available, experimental data are summarized and analyzed. Under specific considerations are ASME Code Case 1441 published in December 1969 and certain revisions which are being considered for adoption by ANSI B31.7 - the nuclear power piping section of the American National Standards Institute Standard Code for Pressure Piping. In this report fatigue failure data obtained from the published literature are compared with design values calculated according to the rules of Code Case 1441 and the stress index analysis method of the 1969 edition of the piping code USAS B31.7-1969. It is shown that the proposed rules are adequately conservative for those components loaded with a cyclic moment, with the possible exception of girth butt welds where additional test data are needed. It is also pointed out that additional test data are needed for longitudinal welds and for components loaded with combinations of internal pressure and bending moments.

Keywords: fatigue, stress indices, nuclear piping, welds, piping tees, piping elbows, pressure vessel nozzles, piping code, ANSI B31.7, pressure vessel code, ASME B and PV Section III, Code Case 1441.



NOMENCLATURE

Stress Indices and Stress Intensification Factor

C_1	=	stress index for pressure loading
C_2	=	stress index for moment loading
C_{2b}	=	stress index for moment loading on branch of tee
K_1	=	stress index for pressure loading
K_2	=	stress index for moment loading
K_{2b}	=	stress index for moment loading on branch of tee
K_3	=	stress index for thermal gradient loading
i	=	fatigue-based stress intensification factor as used in B31.1.0

Stresses

S_n	=	primary plus secondary stress range as calculated by Equation (10) of B31.7, Equation (1) herein
S_p	=	total stress range as calculated by Equation (11) of B31.7, Equation (2) herein
S_a	=	S_{alt} = total stress amplitude
S_m	=	allowable stress intensity for material and temperature as given in Table A.1 of B31.7
S	=	equivalent stress amplitude
S_A	=	allowable expansion stress per B31.1.0
S_c	=	basic allowable stress at minimum (cold) temperature per B31.1.0
S_h	=	basic allowable stress at maximum (hot) temperature per B31.1.0
S_ℓ	=	longitudinal stress as defined in B31.1.0

Cycles of Loading

- N_c = design cycles calculated using B31.7 indices/Case 1441 method
 N_t = experimentally determined cycles to failure (through-the-wall crack)
 N = cycles to failure predicted by Equation (20)
 N_D = design cycles by Equation (23) with factor of safety of 2 on stress

Loads

- P_o = internal pressure range
 M = moment loading range
 M_i = moment loading vector range

Dimensions & Dimensional Parameters

- D_o = nominal outside diameter of component
 t = nominal wall thickness of component
 I = moment of inertia of component cross section, based on nominal dimensions
 Z = section modulus of component cross section, based on nominal dimensions
 r = nominal mean cross section radius of a component (run size for forged welding tees)
 h_2 = tR/r^2 , where R = bend radius of butt welding elbow

B31.7 Symbols for Branch Connections
per Par. 1-704.3

R	=	mean radius of run pipe
T	=	nominal wall thickness of run pipe
r	=	mean radius of branch pipe
r_p	=	radius of reinforcing pad

Symbols Used in Thermal Gradient Analysis

E	=	modulus of elasticity
α	=	coefficient of thermal expansion
ν	=	Poisson's ratio
Bi	=	$h\delta/K$
Fo	=	α_d/δ^2
h	=	film coefficient, Btu/hr-ft ² -°F
δ	=	plate thickness, ft.
K	=	thermal conductivity of plate material, Btu/hr-ft-°F
α_d	=	thermal diffusivity of plate material, ft ² /hr
θ	=	time, hours
\bar{T}	=	average temperature through wall thickness
ΔT_1	=	linear portion of temperature gradient through wall, °F
ΔT_2	=	non-linear portion of temperature gradient through wall, °F
T_o	=	outside surface temperature, °F
T_i	=	inside surface temperature, °F
T_a	=	magnitude of step fluid temperature change, °F

Symbols Used in Fatigue Analysis with $S_n > 3S_m$

K_e	=	factor defined by Equation (3) herein
m,n	=	material dependent constants

LIST OF TABLES

	<u>Page</u>
Table 1. Evaluation of Fatigue Tests on Girth Butt Welds with Cyclic Moment Loadings	10
Table 2. Evaluation of Fatigue Tests on Short-Radius and Long-Radius Elbows	14
Table 3. Evaluation of Fatigue Tests on Forged Welding Tees with Moment Loading	18
Table 4. Evaluation of Fatigue Tests on Fabricated and Drawn Outlet Tees with Cyclic Moment Loading	20
Table 5. Evaluation of Fatigue Tests on Girth Fillet Welds with Moment Loading	23
Table 6. Evaluation of General Electric Tests on 6-Inch Notched Pipe with a Theoretical Stress Concentration Factor of 3.6, Moment Loading	26
Table 7. Evaluation of Cyclic Pressure Fatigue Tests on Nozzles in Pressure Vessels, Test Data from Reference (14)	30
Table 8. Dimensions and Material Data, Reference (15) Nozzles in Cylindrical Vessels	34
Table 9. Evaluation of Cyclic Pressure Tests on Nozzles in Cylindrical Pressure Vessels, Data from Reference (15)	35
Table 10. Evaluation of Cyclic Pressure Tests on Longitudinal Butt Welds in Cylindrical Pressure Vessels, Data from Reference (15)	37

COMPARISONS OF TEST DATA WITH CODE METHODS
FOR FATIGUE EVALUATION

INTRODUCTION

The design analysis prescribed in both the Nuclear Vessels Code, ASME Boiler Code, Section III⁽¹⁾, and the Nuclear Piping Code, USAS B31.7-1969⁽²⁾, involve a limit to the primary plus secondary stress intensity range of $3S_m$. The value of S_m is essentially* limited to two-thirds of the yield strength of the material; hence, the $3S_m$ limit is equivalent to a $2S_y$ limit, where S_y is the material yield strength. This limit is related to "shake-down" concepts; i.e., if the primary plus secondary stress-intensity range, denoted as S_n herein, is less than $3S_m$, then the strain range can be obtained by an elastic stress analysis and the fatigue life can be determined by comparison of the strain range obtained from the elastic analysis.

However, if S_n exceeds $3S_m$, the fatigue life of the component is not necessarily negligible, as will be shown by test data cited herein. These data suggest that components may be safely used with $S_n > 3S_m$ provided that the fatigue analysis method accounts for the plastic strain range which may occur under such conditions. One might, in principal, conduct an elastic-plastic analysis of the component. In practice, however, a reasonably accurate elastic-plastic analysis, even for a relatively simple component such as a curved pipe, is a formidable undertaking; particularly if several loadings (e.g., internal pressure, moments, thermal gradients) are involved as is often the case with piping components.

It is apparent that a simple yet conservative adjustment to an elastic analysis for application to the fatigue analysis of components when $S_n > 3S_m$ is needed. This kind of an adjustment is included in USAS B31.7; 1-705.4, "Simplified Elastic-Plastic Discontinuity Analysis". Phase Report 115-2, "Comparison of USAS B31.7 Plastic Fatigue Analysis With Test Data on Piping Components"⁽³⁾, gives a comparison of test data with this fatigue analysis method.

* For certain materials, S_m at temperature may be up to 90 percent of S_y . However, because of the strain-hardening characteristics of these materials, $3S_m$ may be deemed as equivalent to $2S_y$ in conjunction with a shake-down analysis assuming no strain hardening.

During the preparation of USAS B31.7, numerous consultations occurred between ASME Section III representatives and B31.7 representatives concerning the simplified elastic-plastic discontinuity analysis method and alternates thereto. Primarily as the result of work by S. W. Tagart, representing B31.7, and B. F. Langer, representing ASME Section III, a modified procedure was worked out which was deemed acceptable to both codes and which was published as ASME Code Case 1441, December 29, 1969. This code case is shown herein as page A-1 of Appendix A. Certain modifications of this code case are now under consideration; those modifications are indicated on page A-2 of the Appendix. USAS B31.7 is in the process of adopting ASME Code Case 1441 to replace the present paragraph 1-705.4.

The purpose of this report is to compare the fatigue analysis method of Code Case 1441 with fatigue tests on piping components in which the test loadings gave secondary stresses which exceeded $3S_m$. The method is used in conjunction with stress indices given in USAS B31.7-1969 and, as such, constitute an evaluation of the stress indices and analysis method; not the analysis method by itself. No implication is intended that the test data are sufficiently broad in scope to confirm the validity of the indices method for all possible piping components, materials, and types of loadings.

Included in the comparisons are:

Cyclic Loading	Component
Moment	Girth butt welds Short and long radius butt welding elbows Forged butt welding tees Fabricated and drawn outlet tees Girth fillet welds
Internal Pressure	Nozzles in cylindrical shells Longitudinal butt welds in cylindrical shells
Thermal Gradient (Step fluid temperature change)	Girth butt welds Forged butt welding tee

EVALUATION PROCEDURE

The evaluation procedure involves B31.7 Equations (10), (11), and the fatigue design graphs (S-N curves) from B31.7/ASME Section III. The design graphs involved in the evaluation are Figures 1-705.3.3(a) and 1-705.3.3(b); included herein as Figures 1 and 2. Four steps, as discussed below, are involved in the evaluation.

(1) Based on the dimensions and loading of the test specimen, a value of S_n was calculated by Equation (10) of B31.7; this equation is:

$$S_n = C_1 \frac{P_o D_o}{2t} + C_2 \frac{D_o}{2I} M_i + \text{thermal stress terms} \quad (1)$$

where S_n = primary plus secondary stress-intensity range
 C_1 = primary plus secondary stress index for pressure loading
 P_o = internal pressure range
 D_o = nominal outside diameter of component
 t = nominal wall thickness of component
 C_2 = primary plus secondary stress index for moment loading
 M_i = moment loading vector range
 I = moment of inertia of component cross section, based on nominal dimensions.

Fatigue test data are available on piping components subjected to either cyclic pressure or cyclic moments; no data are available on combined cyclic pressure with cyclic moments, although some of the cyclic moment tests were carried out with a nonzero, but constant, internal pressure.

(2) A value of S_p was calculated by Equation (11) of B31.7; this equation is:

$$S_p = K_1 C_1 \frac{P_o D_o}{2t} + K_2 C_2 \frac{D_o}{2I} M_i + \text{thermal stress terms} \quad (2)$$

where K_1 = peak stress index for pressure loading.
 K_2 = peak stress index for moment loading.

Other symbols are defined under Equation (1). One set of test data are available for evaluation of the thermal stress terms in Equations (1) and (2); these terms will be defined where used in the evaluation (see "Thermal Gradient Loading").

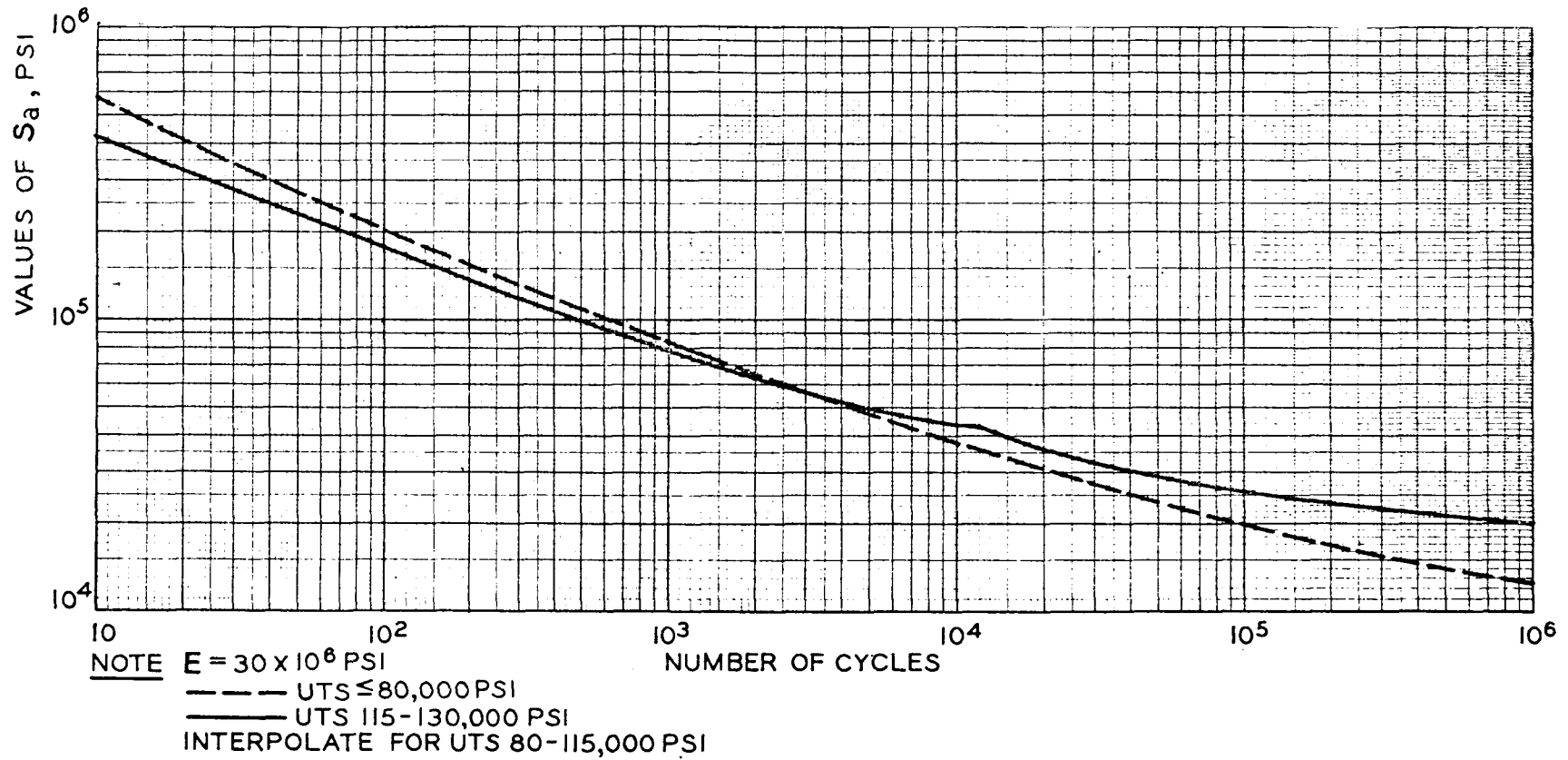


FIGURE 1. ALLOWABLE AMPLITUDE OF ALTERNATING STRESS INTENSITY, S_a , FOR CARBON AND ALLOY STEELS WITH METAL TEMPERATURES NOT EXCEEDING 700°F, FROM B31.7, FIGURE 1-705.3.3(a)

(3) Most of the test data selected for evaluation involved components and loads such that S_n was greater than $3S_m$. The next step in the analysis, therefore, consisted of the calculation of K_e (Code Case 1441, see Appendix A) by the equation:

$$K_e = 1.0 + \frac{1-n}{n(m-1)} \left(\frac{S_n}{3S_m} - 1 \right); 1.0 \leq K_e \leq 1/n \quad (3)$$

where m and n are material-dependent parameters as listed below for the materials evaluated in this report.

Material	m	n	K_e	$(K_e)_{\max}$
Carbon steel	3.0	0.2	$1 + 2 [(S_n/3S_m) - 1]$	5.0
Austenitic stainless steel	1.7	0.3	$1 + 3.33 [(S_n/3S_m) - 1]$	3.33
Low-alloy steel	2.0	0.2	$1 + 4 [(S_n/3S_m) - 1]$	5.0

(4) S_{alt} was calculated by:

$$S_{alt} = \frac{K_e S_p}{2} \quad (4)$$

The value of N_c corresponding to $S_{alt} = S_a$ was then determined from Figures (1) or (2) herein. Values of N_t/N_c are shown in the comparisons. In this report, N_t represents the number of cycles to produce a crack through the wall of the component.*

The "design" S-N curves, Figures 1 and 2 herein, were obtained from the "failure" S-N curves by applying a factor of two on stress or a factor of 20 on life, whichever was more conservative at each point.⁽¹⁾ Accordingly, in the writers' opinion, a ratio of $N_t/N_c \geq \sim 20$ indicates adequate conservatism of the code indices method.

* References (6) and (8) give data on cycles to initiation of macroscopic cracks and Reference (8) also gives data on the growth rate of the cracks.

MOMENT LOADING

Test data for moment loading fatigue tests of piping components from References 4 through 9, and notched pipe tests from Reference 8 are discussed in this section. The evaluation of these tests involve the second term of Equations (1) and (2); these are:

$$S_n = C_2 \frac{D_o}{2I} M_i = C_2 \frac{M_i}{Z} \quad (5)$$

where $Z = \text{nominal section modulus} = 2I/D_o$

$$S_p = K_2 C_2 M_i / Z \quad (6)$$

In general, M_i is the vector sum of an orthogonal set of moments applied to a component. However, in the fatigue tests included herein, only one moment was applied in any given test; therefore, M_i is simply the range of that applied moment.

The tests of References (4), (5), (7), and (9) were constant displacement tests; the equivalent moment was obtained by extrapolation of the elastic moment-displacement relationship to the test-imposed displacement. Accordingly, these tests produced stresses of the "secondary-stress" category which, by definition, are displacement imposed stresses. Reference (6) tests, in contrast, were constant moment (load-controlled) tests; B31.7 limits such loads to a stress limit of $1.5 S_m$ by Equation (9) of B31.7. Reference (8) tests were displacement controlled, but the reported loads were not extrapolated from the elastic moment-displacement relationship but represent the measured "shakedown force". This force is presumably somewhat less than the extrapolated force; use of the shakedown force in evaluation is conservative* because the B31.7 indices method is based on elastic stress calculations.

Actually, B31.7 independently restricts expansion stresses [corresponding to controlled displacement tests of References (4), (5), (7), and (8)]

* Note that if the extrapolated force is higher than the shakedown force, then M/Z , on an elastic basis, would be higher than those tabulated from Reference (8); N_c would then be lower and N_t/N_c a higher ratio.

to $3S_m$ by Equation (12) of B31.7; accordingly, all of the tests discussed in this section for piping components and most of the tests on notched pipe were under loadings more severe than permitted by B31.7. No attempt is made herein to completely describe the test specimens or test procedure; the interested reader should consult the references cited for these details.

Girth Butt Welds

Evaluation of tests on girth butt welds are summarized in Table 1. Markl's⁽⁴⁾ tests represent what may be considered as typical welds in A106 Grade B pipe made by a good welder. Additional bending fatigue tests on girth butt welds in pipe are given in References (10), (11), (12), and (13). These data fairly well confirm Markl's results for typical butt welds and also give indications of the improvement in fatigue life for, in particular, a weld with a smooth inside surface. These additional tests were run at lower nominal stresses; hence, they are not of direct interest in the present comparisons for $S_n > 3S_m$.

As analyzed by the B31.7 procedure, a C_2 -factor of 1.0 and a K_2 -factor of 1.8 is assigned. For comparison purposes, a group of three test results were selected which were run at highest nominal stresses; i.e., at a nominal stress amplitude of 45,000 psi. Markl's tests were all run with completely reversed displacements; hence, the nominal stress amplitude [shown in Reference (4)] must be doubled and multiplied by C_2 to obtain the B31.7 computed stress range, S_n . For girth butt welds, $C_2 = 1.0$; hence, S_n is simply the nominal stress range shown in Table 1 as M/Z . S_m is taken as 20,000 psi (A106 Grade B at room temperature) and $S_n/3S_m = 90,000/60,000 = 1.5$

The value of S_p , from Equation (6), is

$$S_p = K_2 C_2 M/Z = 1.8 \times 1.0 \times 90,000 = 162,000 \text{ psi.}$$

The value of K_e , from Equation (3) for carbon steel, $m = 3$, $n = 0.2$, is

$$K_e = 1 + \frac{0.8}{0.2 \times 2} (1.5 - 1) = 2.0$$

and, from Equation (4),

$$S_{alt} = \frac{2.0 \times 162,000}{2} = 162,000 \text{ psi.}$$

Entering Figure 1.705.3.3(a) of B31.7 (Figure 1 herein) with $S_{alt} = S_a = 162,000$, the value of N_c , design cycles per B31.7, is found to be about 190. This is compared in Table 1 with test cycles-to-failure, N_t , of 2500 to 3500. The last column of Table 1 shows values of N_t/N_c from 13 to 18 for the tests taken from Reference (4).

TABLE 1. EVALUATION OF FATIGUE TESTS ON GIRTH BUTT WELDS WITH CYCLIC MOMENT LOADINGS

Ref. No.	Type of Component	$\frac{M}{Z}$	S_n	$\frac{S_n}{3S_m}$	S_p	K_e	$\frac{K_e S_p}{2}$	B31.7 N_c	Test N_t	$\frac{N_t}{N_c}$
(4) Fig. 5	Girth butt weld 4" std. wt.	90,000	90,000	1.50	162,000	2.00	162,000	190	2,500 to 3,500	13 to 18**
(8) HW-1	Girth butt weld 6" std. wt.	58,200	58,200	1.08	105,000	1.16	60,800	2500	35,740	14.3
(8) HWD-1	Girth butt weld* 6" std wt.	59,200	59,200	1.10	107,000	1.20	64,200	2000	13,600	6.8*
(8) HW-3A	Girth butt weld 6" std. wt.	61,100	61,100	1.272	110,000	1.905	105,000	1100	6,950	6.3
(8) HWD-3	Girth butt weld* 6" std. wt.	59,900	59,900	1.247	107,800	1.823	98,500	1400	2,600	1.9*

* Specimen had an intentional defect, see text.

** Range of N_t/N_c for three test specimens.

Four tests from Reference (8) on girth butt welds are shown in Table 1. These are classified as:

<u>Identification</u>	<u>Pipe Material</u>	<u>Weld</u>	<u>Test Temperature</u>
HW-1	Al06B, carbon steel	Good	550 F
HWD-1	Al06B, carbon steel	Defective	↓
HW-3A	304 stainless steel	Good	
HWD-3	304 stainless steel	Defective	

The "defective" welds had an intentional defect; a lack of penetration produced by not completing a 1-inch section of root pass. Presumably the defect was aligned with the maximum bending stress during the test.

The cycles-to-failure of HW-1 agrees well with Markl's⁽⁴⁾ equation for girth butt welds in Al06B carbon steel type at room temperature; i.e.

$$\frac{1}{2} \frac{M}{Z} = 245,000 N^{-0.2} \quad (7)$$

Equation (7) gives $N = 42,300$ at $M/Z = 58,200$ psi, as compared to $N_t = 35,740$ for HW-1.*

Equation (7) gives $N = 33,200$ at $M/Z = 61,100$ psi, as compared to $N_t = 6950$ for HW-3A (stainless at 550 F). On the basis of room temperature fatigue properties of carbon steel versus stainless steel, it is surprising to find that the carbon steel weld (HW-1) was better than the stainless steel weld (HW-3A). For example, Markl⁽²⁰⁾ suggests that the constant of 245,000 in Equation (7) should be 281,000 for Type 316 stainless steel at room temperature.

However, it is significant to note that the trend of the relationship obtained by the tests at 550 F is predicted by K_e as shown by the following tabulation where M/Z is assumed to be 60,000 psi.

* The agreement, however, may be fortuitous. Note that M/Z in Markl's tests and in the B31.7 procedure is an elastic basis range whereas the values of M/Z from Reference (8), for lack of more pertinent data therein, represent a shake-down force range.

	Room Temperature		550 F	
	<u>Carbon</u>	<u>Stainless</u>	<u>Carbon</u>	<u>Stainless</u>
S_m	20,000	20,000	18,000	16,000
K_e	1.0	1.0	1.222	1.833
$K_{e p} S_e / 2$	54,000	54,000	66,000	99,000
N_c	3,500	14,000	1,800	1,350

While the above tabulation does not quantitatively agree with the relative test results at 550 F (i.e., 35,740/6,950 test versus 1800/1350 calculated) it does indicate that a relatively lower fatigue life for stainless as compared to carbon steel, both at 550 F, might be expected.*

The reduction in fatigue life by the defect was essentially the same for carbon steel as for stainless steel; i.e., $35,740/13,600 = 2.63$ versus $6,950/2,600 = 2.67$. Assuming that N is proportional to $(1/S)^5$, the effective stress intensification factor due to the defect is $(2.65)^2 = 1.22$. In terms of B31.7 stress indices, a K_2 -index of $1.8 \times 1.22 = 2.20$ is indicated by these particular test results.

As shown by the last column of Table 1, the value of N_t/N_c ranges from 13 to 18 for "good" or "typical" welds in A106B carbon-steel pipe at room temperature and one test at 550 F. These values of N_t/N_c are, in the writer's opinion, acceptable but do not indicate any excess conservatism in the B31.7 indices method.

The single test of a "good" girth-butt weld in 304 stainless-steel pipe at 550 F (HW-3A) gave $N_t/N_c = 6.3$. This isolated test result is somewhat disturbing and should be confirmed by additional tests. If the available test turns out to represent a low side of the scatter band, it might be concluded that no change is needed in the B31.7 indices method. If however, the available test represents a mean (or possibly even a high point) some adjustment to the B31.7 indices method for stainless steel at higher than room temperature would seem to be necessary to maintain a reasonable design factor of safety.

* However, the correlation indicated arises entirely from K_e . If $M/Z = 48,000 = S_n$, then the B31.7 (and ASME III) analysis would predict that stainless would be better than carbon steel both at room temperature and at 550 F and the fatigue life would not depend upon temperature. Test data to evaluate this seeming anomaly would be highly desirable.

Short Radius and Long Radius Elbows

The C_2 -indices for the elbows listed in Table 2 were obtained by the equation given in B31.7, Appendix D, Table D-201:

$$C_2 = \frac{1.95}{h_2^{2/3}} \quad (8)$$

where $h_2 = tR/r^2$
 t = nominal elbow wall thickness
 R = bend radius of elbow
 r = mean elbow cross-section radius.

The C_2 -indices, for the elbows included in Table 1, are tabulated below:

Elbow	r	R	t	h	C_2
4-inch, standard wt., short radius	2.131	4.00	0.237	0.209	5.54
4-inch, 0.072-inch wall, short radius	2.214	4.00	0.072	0.0588	12.9
6-inch, standard wt., short radius	3.172	6.00	0.280	0.167	6.43
4-inch, standard wt., long radius	2.131	6.00	0.237	0.313	4.23
4-inch, 0.101-inch wall, long radius	2.200	6.00	0.101	0.125	7.79
6-inch, standard wt., long radius	3.172	9.00	0.280	0.250	4.91

The constant of 1.95 in Equation (8) is such that, for any set of orthogonal moments, the value of $C_2 M_i / Z$ is not unconservative. For either in-plane or out-of-plane moment loading, the maximum elastic stresses are lower than indicated by Equation (8).

B31.7 assigns a K_2 -index of unity to elbows of the type tested; i.e., seamless elbows with no connections, attachments, or other extraneous raisers on the bodies thereof.

Table 2 lists 12 comparisons, taken from Reference (4) and (5), between either single tests or groups of tests at about the same nominal stress level. These particular tests were selected from the figures cited as representing highest test values of S_n . These are all tests on specimens made from A106 Grade B material; all were run at room temperature and all but two were

TABLE 2. EVALUATION OF FATIGUE TESTS ON SHORT-RADIUS AND LONG-RADIUS ELBOWS

Ref. No.	Type of Component	$\frac{M}{Z}$	S_n	$\frac{S_n}{3S_m}$	S_p	K_e	$\frac{K_e S_p}{2}$	B31.7 N_c	Test N_t	$\frac{N_t}{N_c}$
(4) Fig. 6	Short-radius elbow 4" std. wt.	100,000	554,000	9.24	554,000	5.00	1,380,000	<<10	300 to 350	>>30
(4) Fig. 6	Short-radius elbow 4" std. wt.	56,000	310,000	5.17	310,000	5.00	775,000	<10	1,200 to 3,000	>120
(4) Fig. 6	Short-radius elbow 0.072" wall	20,000	250,000	4.17	250,000	5.00	625,000	~10	2,800	~280
(4) Fig. 7	Short-radius elbow 4" std. wt.	56,000	310,000	5.17	310,000	5.00	775,000	<10	2,800	>280
(4) Fig. 7	Short-radius elbow 0.072" wall	30,000	375,000	6.25	375,000	5.00	935,000	<10	5,000	>500
(4) Fig. 7	Short-radius elbow 0.072" wall	20,000	250,000	4.17	250,000	5.00	625,000	~10	15,000	~1500
(8) CCLS-1	Short-radius elbow 6" std. wt.	43,600	280,000	4.67	280,000	5.00	700,000	<10	1,176	>118
(8) CCLS-2	Short-radius elbow 6" std. wt.	42,600	274,000	4.57	274,000	5.00	685,000	<10	7,899	>790
(8) CSLS-2	Short-radius elbow 6" std. wt.	42,200	272,000	4.54	272,000	3.33	454,000	22	6,838	310
(8) CSLS-1	Short-radius elbow 6" std. wt.	44,200	284,000	4.75	284,000	3.33	473,000	20	907	45

TABLE 2. (Continued)

Ref. No.	Type of Component	$\frac{M}{Z}$	S_n	$\frac{S_n}{3S_m}$	S_p	K_e	$\frac{K_e S_p}{2}$	B31.7 N_c	Test N_t	$\frac{N_t}{N_c}$
(8) HCLS-1	Short-radius elbow 6" std. wt.	43,500	280,000	5.20	280,000	5.00	700,000	<10	760	>76
(8) HCLS-2	Short-radius elbow 6" std. wt.	43,100	278,000	5.15	278,000	5.00	695,000	<10	26,100	>2600
(8) HSLs-1	Short-radius elbow 6" std. wt.	28,000	180,000	3.75	180,000	3.33	300,000	56	2,200	39
(8) HSLs-2	Short-radius elbow 6" std. wt.	42,200	271,000	5.65	271,000	3.33	452,000	22	1,870	85
(4) Fig. 8	Long-radius elbow 4" std. wt.	50,000	212,000	3.54	212,000	5.00	530,000	12	2,500 to 20,000	210 to 1700
(4) Fig. 8	Long-radius elbow, 4" 0.10" wall	24,000	179,000	2.98	179,000	4.96	445,000	17	2,000	118
(4) Fig. 9	Long-radius elbow 4" std. wt.	86,000	365,000	6.08	365,000	5.00	910,000	<10	2,500	>2500
(4) Fig. 9	Long-radius elbow, 4" 0.101" wall	29,000	216,000	3.60	216,000	5.00	540,000	11	5,000	450
(8) CSLS-3	Long-radius elbow 6" std. wt.	44,200	217,000	3.62	217,000	3.33	362,000	35	4,469	128
(5) Fig. 7	Long-radius elbow, 4" std wt., P = 2200	74,000	313,000	5.21	313,000	5.00	785,000	<10	1,300	>130
(5) Fig. 8	Long radius elbow, 4" std. wt., P = 2200	80,000	338,000	5.64	338,000	5.00	845,000	<10	700	>70

run with zero internal pressure; these two were run with an internal pressure of 2200 psi as indicated in Table 2 by "P = 2200".

In addition to the tests taken from Reference (4) and (5), results of 9 tests from Reference (8) are shown in Table 2. The test temperature and material are identified by the first two letters in the specimen identification, i.e.,

First letter C = test run at room temperature

H = test run at 550 F

Second letter C = carbon steel material, ASTM A234, Grade WPB

S = type 304 stainless steel.

All tests from Reference (8) at room temperature were run with an internal pressure of 1050 psi; all tests at 550 F were run with zero internal pressure.

Examination of the last column of Table 2 indicates that the ratio of N_t/N_c is always greater than 20.

Forged Welding Tees

The C_{2b} -indices for the forged welding tees (ASA B16.9 tees) listed in Table 3 were obtained by the equation given in B31.7 Appendix D, Table D-201:

$$C_{2b} = 0.67(r/t)^{2/3} \quad (9)$$

where t = nominal wall thickness of run of tee
 r = mean cross-section radius of run of tee.

The C_{2b} -indices for the tees included in Table 3 are:

<u>Run of Tee</u>	<u>r</u>	<u>t</u>	<u>C_{2b}</u>
4-inch, std. wt.	2.131	0.237	2.90
6-inch, std. wt. and Sch. 40	3.172	0.280	3.38
12-inch, Sch. 40	6.172	0.406	4.11
12-inch, Sch. 80	6.031	0.687	2.85
12-inch, Sch. 160	5.719	1.312	1.79
24-inch, Sch. 40	11.656	0.687	4.42

Equation (9) is intended to be such that conservative results are obtained regardless of what combination of moments is applied. (Six independent moments can be applied to a tee.) The moments used in the tests are not necessarily those which give highest stresses per unit moment.

B31.7 assigns a K_2 -index of unity to tees of the type tested.

All of the tests listed in Table 3 were run at room temperature.

Tests were run with constant internal pressure of:

<u>Reference</u>	<u>Internal Pressure</u>
(4)	Zero
(8)	1050 psi
(9)	Design pressure calculated by Equation (2) of B31.7, with $t_m = 0.875$ times nominal wall thickness of the run pipe and $a = 0$.

The last column of Table 3 shows $N_t/N_c > 20$ for all of the forged welding tees.

TABLE 3. EVALUATION OF FATIGUE TESTS ON FORGED WELDING TEES WITH MOMENT LOADING

Ref. No.	Type of Component (1)	$\frac{M}{Z}$ (2)	S_n	$\frac{S_n}{3S_m}$	S_p	K_e	$\frac{K_e S_{e-p}}{2}$	B31.7 N_c	Test N_t	$\frac{N_t}{N_c}$
(4) Fig. 10	Forged welding tee 4" std. wt.	100,000	290,000	4.85	290,000	5.00	725,000	< 10	900	> 90
(4) Fig. 10	Forged welding tee 4" std. wt.	86,000	250,000	4.17	250,000	5.00	625,000	~ 10	1,500 to 5,000	150 to 500
(4) Fig. 11	Forged welding tee 4" std. wt.	104,000	300,000	5.00	300,000	5.00	750,000	< 10	1,500	> 150
(4) Fig. 11	Forged welding tee 4" std. wt.	86,000	250,000	4.17	250,000	5.00	625,000	< 10	700 to 4,000	> 70
(8) CSTS-1	Forged welding tee* 6" std. wt.	68,700	232,000	3.87	232,000	5.00	580,000	~ 10	4,575	~ 460
(8) CSTS-2	Forged welding tee* 6" std. wt.	67,800	229,000	3.84	229,000	5.00	574,000	~ 10	3,310	~ 330
(9) T-4	Forged welding tee 12" Sch. 80	54,500	155,000	2.57	155,000	4.14	321,000	38	2,070	55
(9) T-7	Forged welding tee* 12" Sch. 160	76,300	137,000	2.28	137,000	3.33	228,000	110	11,475	104
(9) T-8	Forged welding tee* 12" x 6" Sch. 40	74,600	307,000	5.12	307,000	3.33	511,000	16	8,249	510
(9) T-10	Forged welding tee 24" Sch. 40	44,000	194,000	3.23	194,000	5.00	485,000	15	18,532	1,200
(9) T-15	Forged welding tee* 12" x 6" Sch. 40	72,300	297,000	4.95	297,000	3.33	495,000	18	11,803	660

(1) All tees were ASTM A106 Gr. B. carbon steel material, except those with an asterisk; these were Type 304 austenitic stainless steel material.

(2) Z is the section modulus of the branch pipe for those tees in which the branch is smaller than the run.

Fabricated and Drawn Outlet Tees

B31.7, Appendix D, gives stress indices for branch connections per Subdivision 1-704.3 which are limited in application to branch connections in which $d/D \leq 0.5$. Three test results are available on tees which "almost" meet these B31.7 restrictions; one fabricated and two with drawn outlets. The evaluation of these tests is summarized in Table 4.

Reference (6) gives the results of a cyclic bending test on a model almost within the d/D limitation. This model, identified as Model R in Table 4, consisted of a 20-inch OD x 1-inch wall run pipe with a 12.75-inch OD x 0.687-inch wall branch pipe.

The test was run with cyclic moments applied on the branch. The C_2 -index for moment loading on the branch is identified as C_{2b} , and is given in B31.7, Appendix D, by the equation:

$$C_{2b} = 3(R/T)^{2/3} (r/R)^{1/2} (t/T) (r/r_p) \quad (10)$$

where R = mean radius of run pipe
 T = nominal thickness of run pipe
 r = mean radius of branch pipe
 t = nominal thickness of branch pipe
 r_p = radius of reinforcing pad.

For Model R, $R = 9.5$, $T = 1.00$, $r = 6.031$, $t = 0.687$, and r_p is appropriately taken as half of the branch pipe outside diameter; $r_p = 6.375$. The value of C_{2b} , by Equation (10), is:

$$C_{2b} = 3(9.5/1.0)^{2/3} (6.031/9.5)^{1/2} (0.687/1.0) (6.031/6.375) = 6.98.$$

B31.7 assigns a K_2 -index of unity to this type of branch connection.

The material used in the test model was carbon steel but not identified as to ASTM specification; $S_m = 20,000$ psi was therefore assumed in the evaluation. The test was run at room temperature with zero internal pressure. The loading was load-controlled rather than displacement controlled as in all previously cited test data. The value of N_t/N_c is ~ 123 .

TABLE 4. EVALUATION OF FATIGUE TESTS ON FABRICATED AND DRAWN OUTLET TEES WITH CYCLIC MOMENT LOADING

Ref. No.	Type of Component	$\frac{M}{Z}$	S_n	$\frac{S_n}{3S_m}$	S_p	K_e	$\frac{K_e S_p}{2}$	B31.7 N_c	Test N_t	$\frac{N_t}{N_c}$
(6) R	Fabricated tee, 20 x 12	13,440	94,000	1.57	94,000	2.14	100,000	650	~ 80,000	~ 123
(6) L	Drawn outlet tee, 20 x 6	46,600	142,000	2.37	142,000	3.74	266,000	55	95,000	1,700
(6) D	Drawn outlet tee, 20 x 12	26,880	188,000	3.14	188,000	5.00	470,000	15	20,000	1,300

Stress indices are not given in B31.7 for drawn outlet tees. As the nearest approximation, the C_2 -index for fabricated tees was used in the evaluation shown in Table 4. The two test specimens involved in the evaluation are identified in Reference (6) and Table 4, as Models L and D. They are both drawn outlets in 20-inch OD x 1.0-inch wall run pipe. The branch pipe, for Model L, was 6.625-inch OD x 0.432-inch wall; for Model D, 12.75-inch OD x 0.687-inch wall. The tests were run with cyclic moment applied on the branch. The C_{2b} -index for Model D, since it is nominally of the same dimensions as fabricated tee, Model R, is also 6.98. The C_{2b} -index for Model L, by Equation (10), is:

$$C_{2b} = 3(9.5/1.0)^{2/3}(3.096/9.5)^{1/2}(0.432/1.0)(3.096/3.312) = 3.04.$$

The material used in the test models was carbon steel but not identified as to ASTM specification; $S_m = 20,000$ psi was therefore assumed in the evaluation. The tests were run at room temperature with zero internal pressure. The loading was load-controlled. Values of N_t/N_c are 1700 and 1300.

Girth Fillet Welds

Markl and George⁽⁷⁾ give results of tests on fillet-welds made between 4-inch pipe and 300-pound ASA B16.5 flanges. Such fillet welds are assigned a C_2 -index of 1.5, K_2 -index of 2.0 by B31.7, Appendix D. These tests, like those of References (4) and (5), were displacement-controlled and fatigue failure was defined as the occurrence of leakage (crack through the wall).

Evaluation of these tests is shown in Table 5. As indicated by the last column of Table 5, the ratios of N_t/N_c , with one exception, are greater than 20. The one exception consisted of a "minimum" weld, described by the authors of Reference (7) as "the welds....were meant to represent the least weld size and quality compatible with code* requirements, were small (the weld size on hub fillets was of the order of 5/16 inch to 3/8 inch) and of a bead-like, unfinished appearance". One of two such specimens (shown in the first line of Table 5) tested at a nominal stress range of 100,000 psi failed in 87 cycles which is roughly ten times the design cycles obtained from the B31.7 analysis. The other of these two specimens failed at 1200 cycles which is roughly equivalent to 120 times the B31.7 design cycles.

* Piping Code in use around 1949.

TABLE 5. EVALUATION OF FATIGUE TESTS ON GIRTH FILLET WELDS WITH MOMENT LOADING

Ref. No.	Type of Component	$\frac{M}{Z}$	S_n	$\frac{S_n}{3S_m}$	S_p	K_e	$\frac{K S_{e p}}{2}$	B31.7 N_c	Test N_t	$\frac{N_t}{N_c}$
(7) Fig. 7	Fillet-welded girth joint	100,000	150,000	2.50	300,000	4.00	600,000	~ 10	87 to 1,200	8.7 to 120
(7) Fig. 7	Fillet-welded girth joint	90,000	135,000	2.25	270,000	3.50	472,000	16	1,200 to 3,000	190
(7) Fig. 8	Fillet-welded girth joint	116,000	174,000	2.90	348,000	4.80	835,000	< 10	1,200	> 120
(7) Fig. 8	Fillet-welded girth joint	90,000	135,000	2.25	270,000	3.50	472,000	16	339 to 2,800	21 to 170
(7) Fig. 9	Fillet-welded girth joint	116,000	174,000	2.90	348,000	4.80	835,000	< 10	750 to 830	> 75

Notched Pipe

Reference (8) gives fatigue test results on 30 straight pipe test specimens containing a machined notch. These tests are principally concerned with crack initiation and crack growth. The pertinent aspect to this report is the cycles to through-the-wall crack. The testing arrangement is shown schematically in Figure 3.

A stress concentration was provided by machining a notch about 6 inches from the flanged end. The notch was made either on the outside or inside of the pipe, as identified in Table 6 by -I (outside) or -II (inside). Details of the notch are shown in Figure 4. The theoretical stress concentration factor of the notch was 3.62. Miniature strain gages were installed on a specimen, from which the ratio of axial strain in the notch to nominal axial strain was found to be 3.6 to 3.7, in good agreement with the theoretical concentration factor. The displacement was controlled in these tests. Test results, test temperature, materials, and internal pressures are summarized in Table 6.

There are, of course, no stress indices for "notches" given in B31.7. However, following the spirit of B31.7, a C_2 -index of unity and a K_2 -index of 3.6 would be assigned on the assumption that stresses due to the notch were highly localized. The evaluation of these data follows the same general procedure used previously.

The last column of Table 6 gives ratios of test cycles N_t to design cycles, N_c . These vary from 8.6 to 140; the overall average of N_t/N_c is 32. In general, these results indicate satisfactory conservatism of the B31.7 evaluation method. The values of N_t shown in Table 6 are the number of full-range cycles applied to produce a crack through the wall. In addition, subsequent to crack initiation, a variable number of cycles of less-than-full-range were applied; these were probably of the order of one-half of the full range.

ORNL-DWG 71-12534

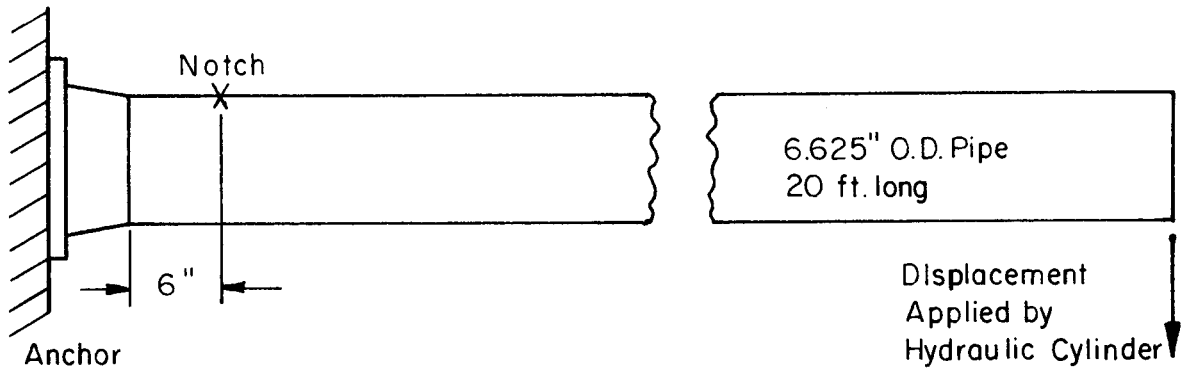


FIGURE 3. REFERENCE (5) FATIGUE TESTS OF NOTCHED PIPE

TABLE 6. EVALUATION OF GENERAL ELECTRIC TESTS ON 6-INCH NOTCHED PIPE WITH
A THEORETICAL STRESS CONCENTRATION FACTOR OF 3.6, MOMENT LOADING

Spec. No. (1)	Material & Sch. (2)	$\frac{M}{Z}$	$\frac{S_n}{3S_m}$	S_p	K_e	$\frac{K_e S_p}{2}$	N_c	N_t	$\frac{N_t}{N_c}$
CSS-3-I	C.S., 40	72,800	1.21	262,000	1.42	186,000	125	1,085	8.7
CSS-4-II	C.S., 40	66,100	1.10	238,000	1.20	143,000	180	4,572	25.
CSS-5-I	C.S., 40	52,800	0.88	190,000	1.00	95,000	700	13,398	19.
CSS-6-II	C.S., 40	77,000	1.28	277,000	1.56	216,000	90	1,453	16.
CSS-7-I	C.S., 80	73,200	1.22	264,000	1.44	190,000	120	1,302	11.
CSS-8-II	C.S., 80	48,800	0.81	176,000	1.00	88,000	900	12,081	13.
CSS-9-I	C.S., 80	45,000	0.75	162,000	1.00	81,000	1000	34,426	34.
CSS-10-II	C.S., 80	40,200	0.67	145,000	1.00	72,500	1500	15,000	10.
CSS-107-I	C.S., 80	74,100	1.24	267,000	1.48	197,600	110	3,575	32.
CSS-109-I	C.S., 80	72,300	1.20	260,000	1.40	182,000	120	4,000	33.
CSS-13-I	C.S., 160	89,000	1.48	320,000	1.96	314,000	37	953	26.
CSS-13-I	C.S., 160	64,000	1.07	230,000	1.14	131,000	220	13,600	62.
HCN-1-I	C.S., 40	52,700	0.98	190,000	1.00	95,000	1500	19,998	13.
HCN-2-I	C.S., 40	75,700	1.40	273,000	1.80	246,000	95	6,520	69.
HCN-3-I	C.S., 40	53,000	0.99	191,000	1.00	95,500	1500	45,237	30.
HCN-4-I	C.S., 40	77,100	1.43	278,000	1.86	259,000	60	3,800	63.

Footnotes are on next page.

TABLE 6. (Contd.)

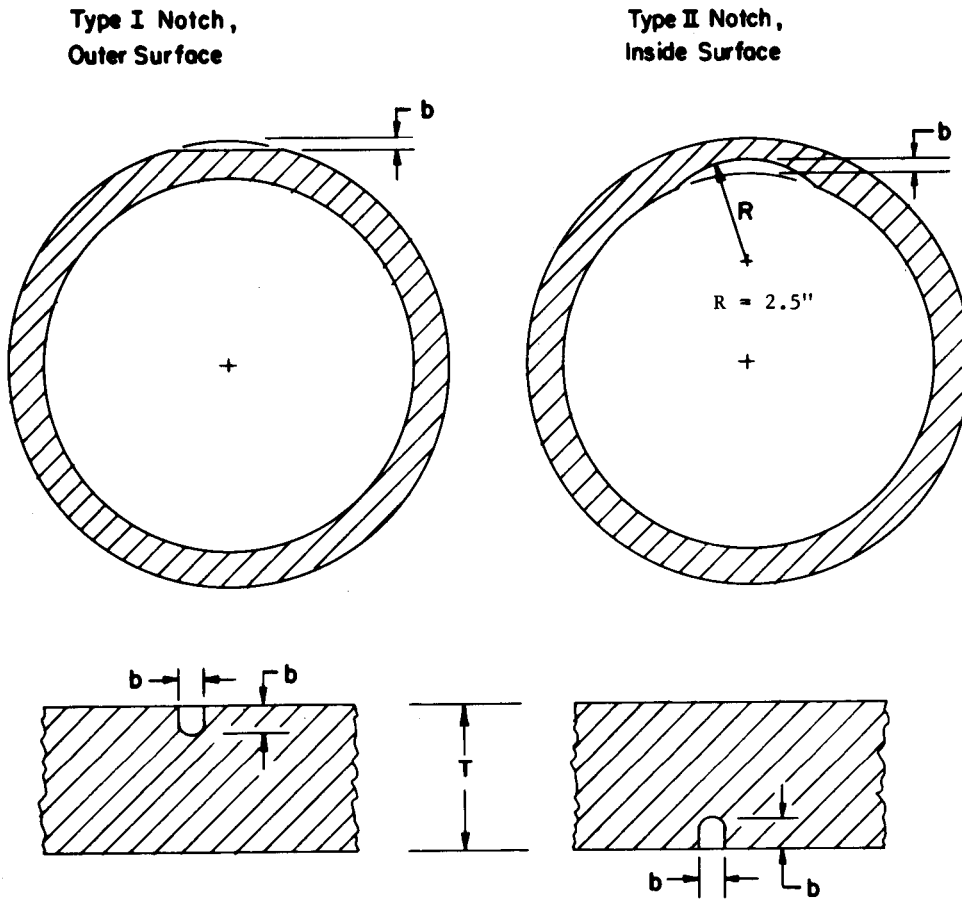
Spec. No. (1)	Material & Sch. (2)	$\frac{M}{Z}$	$\frac{S_n}{3S_m}$	S_p	K_e	$\frac{K S_e p}{2}$	N_c	N_t	$\frac{N_t}{N_c}$
CSS-15-I	S.S., 40	48,300	0.80	174,000	1.00	87,000	2100	20,127	9.6
CSS-16-II	S.S., 80	60,000	1.00	216,000	1.00	108,000	1000	8,596	8.6
CSS-119-I	S.S., 80	74,600	1.24	269,000	1.80	242,000	95	4,656	49.
CSS-23-I	S.S., 160	82,000	1.37	295,000	2.23	329,000	45	1,735	39.
CSS-25-I	S.S., 160	70,500	1.18	254,000	1.60	203,000	150	11,883	79.
HSN-5-I	S.S., 40	57,200	1.19	206,000	1.63	168,000	270	4,701	17.
HSN-1-I	S.S., 40	58,400	1.22	210,000	1.73	182,000	200	4,350	22.
HSNP-1-II	S.S., 80	59,500	1.24	214,000	1.80	193,000	175	4,900	28.
CSS-27-I	A.S., 40	68,300	1.14	246,000	1.47	181,000	130	1,500	12.
CSS-29-I	A.S., 40	52,100	0.87	186,000	1.00	93,000	750	11,950	16.
CSS-31-I	A.S., 80	75,300	1.26	271,000	1.87	253,000	400	4,800	12.
CSS-35-I	A.S., 160	47,500	0.79	171,000	1.00	85,500	950	40,000	42.
CSS-36-II	A.S., 160	46,600	0.78	168,000	1.00	84,000	1000	19,000	19.
CSS-37-I	A.S., 160	91,300	1.52	329,000	2.73	449,000	17	2,365	140.

(1) Specimens with first identification letter C were run at room temperature; H at 550 F. All room temperature tests were run with 1050 psi internal pressure. All 550 F tests were run at zero internal pressure, except HSNP-1-II, for which the internal pressure was 1000 psi. -I indicates outside notch, -II indicates inside notch.

(2) Material identification:

C.S. = A106 Grade B carbon steel
S.S. = A312 Type 304 stainless steel
A.S. = A355 Grade P22, 2-1/4 Cr - 1 Mo steel

ORNL-DWG 71-9091



$b = 0.16T$
T = pipe wall thickness
= 0.280 (Sch 40), 0.432 (Sch 80), 0.718 (Sch 160)

FIGURE 4. DETAILS OF NOTCH USED IN REFERENCE (5) NOTCHED PIPE TESTS

PRESSURE LOADING

Data from cyclic pressure tests on nozzles in cylindrical pressure vessels, and one set of cyclic pressure test data on longitudinal welds in cylindrical pressure vessels are discussed in this section. The latter were an unintended but informative by-product of tests on nozzles in the vessels.

The evaluation of these tests involve the first term of Equations (1) and (2); these are:

$$S_n = C_1 \frac{P_o D_o}{2t} \quad . \quad (11)$$

$$S_p = C_1 K_1 \frac{P_o D_o}{2t} \quad . \quad (12)$$

Nozzles in Pressure Vessels-I

Pickett and Grigory⁽¹⁴⁾ give results of cyclic pressure tests on a series of eight cylindrical pressure vessels containing various types of nozzles. The cylinders were 40-inch OD x 2-inch wall thickness. The vessel material is indicated in Table 7 along with pertinent parameters for comparison of the test data with the B31.7 design procedure.

In these tests, pressure was cycled from zero to the maximum pressure shown in Table 7. The corresponding maximum hoop stress is shown in the fourth column of Table 7. The hoop stress is, of course, a primary stress and is limited by B31.7 to S_m ; i.e., to 20,000 psi for 201-B and 2-1/4 Cr-1Mo; to 26,700 psi for A302-B. This limit is exceeded in all these tests by factors ranging from 1.3 to 2.2.

Reference (14) tests include eight pressure vessels, six of which are listed in Table 7. The other two vessels were made of "T-1" material for which B31.7 does not give allowable stresses. Also, in these two vessels, only one nozzle leakage failure occurred; the other leakage failures occurred in the longitudinal seam weld of the vessel shell or in the vessel shell.

TABLE 7. EVALUATION OF CYCLIC PRESSURE FATIGUE TESTS ON NOZZLES
IN PRESSURE VESSELS, TEST DATA FROM REFERENCE (14)

Vessel No.	Nozzle No.	P_o	$\frac{P D_o}{2t}$	S_n	$\frac{S_n}{3S_m}$	S_p	K_e	$\frac{K S_{ep}}{2}$	B31.7 N_c	Test N_t	$\frac{N_t}{N_c}$
1 (201-B)	11	4,325	43,250	86,500	1.44	147,000	1.88	138,000	200	5,174	26.
	1									7,223	36.
	6									7,516	38.
2 (201-B)	6	2,650	26,500	53,000	0.88	90,000	1.00	45,000	6,000	85,868	14.
	2									123,620	23.
3 (302-B)	1	4,400	44,000	88,000	1.10	150,000	1.40	105,000	550	8,990	16.
4 (302-B)	6	3,460	34,600	69,200	0.87	117,500	1.00	58,750	275	40,041	15.
	11									48,437	18.
7 (201-B)	9B ⁽¹⁾	2,650	26,500	53,000	0.88	90,000	1.00	45,000	(1)	23,908	(1)
	11									135,600	23.
	2N									375,357	62.
2-1/4 Cr-1Mo	1	4,400	44,000	88,000	1.47	150,000	2.88	216,000	85	21,070	25.

(1) Nozzle 9B consisted of a 14.225-inch ID x 0.806-inch wall pipe in an 18-inch ID radius x 1.000-inch wall spherical head. It is essentially an unreinforced nozzle. B31.7 does not give C_1 - or K_1 -indices for this kind of a branch connection.

The comparison shown in Table 7 are for failures at nozzles where the crack penetrated through the wall to produce leakage. The nozzles involved in these failures are identified in Reference (14) and Table 7 by the Numbers 1, 2, 6, 9B, and 11. These nozzles, as well as other nozzles, were placed in one or more of the eight vessels tested. Some comments concerning these nozzle designs are given below.

Nozzle 1. The branch pipe was 10.75-inch OD x 0.593-inch wall thickness. Reinforcing consisted of a weld-on ring. The ring dimensions are not given in Reference (14); however, by scaling from the drawings, it appears that the nozzle has close to 100 percent area replacement reinforcement. However, this would not be an acceptable nozzle under B31.7 (see 1-704.3.3.4(d)). This type of nozzle was used in Vessels 1, 3, 5, and the 2-1/4 Cr-1Mo vessel.

Nozzles 2 and 2N. The branch pipe was 10.75-inch OD x 0.593-inch wall thickness. The nozzle is of the type shown in B31.7, Figure 1-704.3.3.1(a) with $\theta = 14$ degrees. The reinforcement used does give 100 percent area replacement. However, because of the limit to the reinforcing zone given in B31.7 (or ASME Section III), the reinforcing considered as effective is only 36 percent of that required. Accordingly, this model does not meet B31.7 requirements. Nozzles of Type 2 were used in Vessels 1 through 6 and the 2-1/4 Cr-Mo vessel. Nozzles 2 and 2N differ only in that Nozzle 2 was a "set-on" type, while Nozzle 2N was a "set-in" type.

Nozzle 6. The branch pipe was 10.75-inch OD x 0.593-inch wall thickness. The nozzle is of the type shown in B31.7, Figure 1.704.3.3.1(c) with $\theta = 37$ degrees. The reinforcement used is about 80 percent area replacement. Accordingly, it does not meet B31.7 requirements. Nozzles of this type were included in all vessels except Vessel 7.

Nozzle 9B. The branch pipe was 15.84-inch OD x 0.806-inch wall thickness. This nozzle was placed in one of the heads of test vessel No. 7. The head was a spherical shell with 18-inch inside radius x 1-inch wall thickness. This is essentially an unreinforced branch connection in the head. Appendix D of B31.7 does not give stress indices for such nozzles.

Nozzle 11. The branch pipe was 2.375-inch OD x 0.1875-inch wall thickness. This is essentially an unreinforced nozzle. B31.7 permits certain small nozzles to be unreinforced; however, one of the restrictions is that

$$d \leq 0.2 \sqrt{R_m T_r}$$

where d = opening size

R_m = run pipe mean radius

T_r = thickness of run pipe.

For this model, $d = 2$ inches and $0.2 \sqrt{R_m T_r} = 0.2 \sqrt{19 \times 2} = 1.23$ inches.

Accordingly, d is not less than $0.2 \sqrt{R_m T_r}$ and the nozzle does not meet the requirements of B31.7.

While none of the nozzles are in strict accordance with B31.7 Sub-division 1-704.3 requirements, we will nevertheless use the C and K indices listed in Appendix D of B31.7. They are: $C_1 = 2.0$, $K_1 = 1.7$. Table 7 shows the maximum test pressure P_o and the nominal stress $P_o D_o / 2t$. Because the pressure was cycled from 0 to P_o , the secondary stress range is $C_1 P_o D_o / 2t$, or simply twice the nominal stress. The peak stress range is 1.7 times the secondary stress range. Three tests where $S_n < 3S_m$ are also included in Table 7 for general interest.

The last column of Table 7 shows that the value of N_t / N_c is always greater than 14 despite the significant violation of primary stress limits and branch connections which do not fully meet B31.7 requirements.

Nozzles in Pressure Vessels-II

Kameoka, et al⁽¹⁵⁾ give results of tests on the six nozzles in cylindrical vessels listed in Table 8. Nozzle Types^(a) T13 and T*13 failed in the longitudinal seam in the vessel; these will be discussed later. Results for nozzle Types^(a) F13, F*13, T20, and F20 are summarized in Table 9.

B31.7 requires 100 percent area replacement for these nozzles. The approximate percentage of area replacement is:

<u>Nozzle Type^(a)</u>	<u>Percent of Area Replacement</u>	
T13	145.	} Failure in longitudinal butt weld
T*13	094.	
F13	052.	} Failure at inside corner of nozzle
F*13	035.	
T20	067.	
F20	050.	

Accordingly, none of the nozzles listed in Table 9 meet B31.7 requirements. However, the evaluation is based on $C_1 = 2.0$, $K_1 = 1.7$; i.e., the B31.7 indices for nozzles per 1-704.3 of B31.7.

The material used for the nozzles was either ASTM A302B or JIS.SF60; the reference does not indicate which nozzle was made from which material. The evaluation is based on ASTM A302B, $S_m = 26,700$ psi, $m = 2.0$, $n = 0.2$ (low-alloy steel).

The data in Table 9 is analogous to that of Table 7. The tabulated values under $P_o D_o / 2t$ show that the membrane stress was higher than the primary stress limit of $S_m = 26,700$ psi. Despite the violation of the primary stress limit and nozzles which did not fully meet B31.7 requirements, the value of N_t / N_c in Table 9 is always greater than 10.

It can be seen in Table 9 that there is a consistent relationship between $S_n / 3S_m$ and N_t / N_c within any one type of nozzle. This suggests that the K_e -factor may be over-compensating for the effect of plastic straining.

^(a)These are identifications used in Reference (15).

TABLE 8. DIMENSIONS AND MATERIAL DATA, REFERENCE (15)
NOZZLES IN CYLINDRICAL VESSELS

Nozzle Type	Vessel		Nozzles					
	D in.	T in.	D/T	d_i/D	t/T	r_o/T	r_i/T	δ/T
T13	11.63	.512	22.7	0.152	0.815	1.82	0.231	0.915
F13	11.63	.512	22.7	0.152	1.00	0.5	0.315	-0-
T*13	11.63	.512	22.7	0.233	0.815	1.82	0.231	0.915
F*13	11.63	.512	22.7	0.233	1.00	0.5	0.314	-0-
T20	11.60	.788	14.7	0.233	1.04	0.435	0.33	-0-
F20	11.60	.788	14.7	0.233	1.04	0.435	0.33	-0-

Chemical Analysis (%)

Material	C	Si	Mn	P	S	Ni	Cr	Mo	V
ASTM A302B	0.20	0.42	1.15	0.016	0.10	0.65	0.38	0.50	--
JIS. SF60	0.40	0.28	0.68	0.012	0.022	--	--	--	--
FTW60	0.17	0.27	1.18	0.014	0.011	--	--	--	0.072

Tensile Test Data (Average as Tested)

Material	Yield psi	U.T.S. psi	Elong. %	Red. in Area, %
ASTM A302B	72,000	94,000	26.0	62.0
JIS. SF60	51,200	86,700	26.0	35.0
FTW 60	89,600	99,600	32.0	69.0

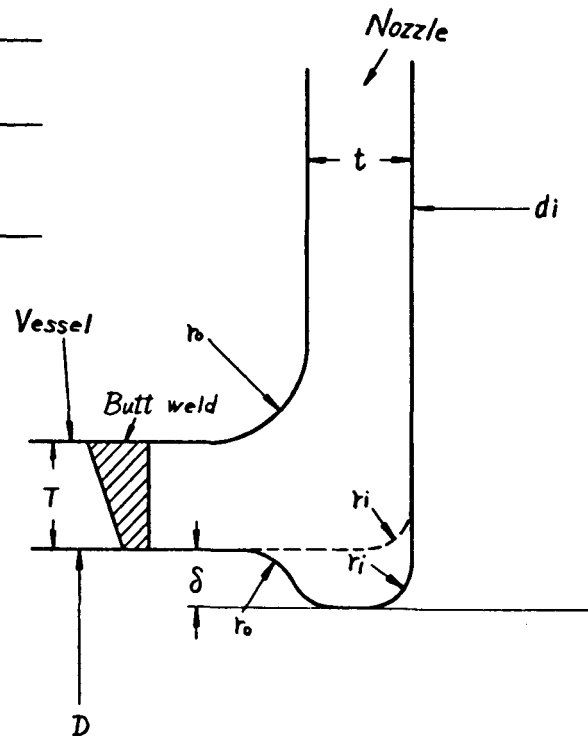


TABLE 9. EVALUATION OF CYCLIC PRESSURE TESTS ON NOZZLES IN
CYLINDRICAL PRESSURE VESSELS, DATA FROM REFERENCE (15)

Nozzle No.	P_o	$\frac{P_o D_o}{2t}$	S_n	$\frac{S_n}{3S_m}$	S_p	K_e	$\frac{K_e S_{e,p}}{2}$	B31.7 N_c	Test N_t	$\frac{N_t}{N_c}$
F13-F	5,400	64,100	128,200	1.61	218,000	3.44	375,000	24	6,518	272.
-D	5,120	60,700	121,400	1.52	206,000	3.08	317,000	38	7,553	198.
-C	4,835	57,300	114,600	1.43	195,000	2.72	265,000	55	9,772	177.
-B	4,270	50,600	101,200	1.265	172,000	2.06	177,000	140	15,553	111.
F*13-1	7,110	84,300	168,600	2.11	287,000	5.00	718,000	<10	2,781	>278.
-4	5,690	67,500	135,000	1.69	229,000	3.76	430,000	10	8,586	859.
-2	5,120	60,700	121,400	1.52	206,000	3.08	317,000	37	14,805	400.
-3	4,270	50,600	101,200	1.265	172,000	2.06	177,000	140	20,505	146.
T20-D	7,820	61,400	122,800	1.53	208,700	3.12	326,000	35	4,376	125.
-A	6,830	53,600	107,200	1.34	182,000	2.36	215,000	90	6,145	68.
-C	6,260	49,000	98,000	1.23	166,600	1.92	160,000	190	9,455	50.
-B	5,690	44,600	89,200	1.12	151,600	1.48	112,000	500	19,032	38.
F20-E	7,110	55,900	111,800	1.40	190,100	2.60	247,000	65	3,462	53.
-F	6,260	49,100	98,200	1.23	166,900	1.92	160,000	190	6,398	34.
-A	5,690	44,600	89,200	1.12	151,600	1.48	112,000	500	14,288	29.
-C	4,835	38,000	76,000	0.95	129,200	1.00	64,500	2000	20,890	10.4

$S_n = 2(P_o D_o / 2t)$, $S_p = 3.4(P_o D_o / 2t)$, $S_m = 26,700$ psi (ASTM A302B).

Longitudinal Butt Welds in Pressure Vessels

As noted in the preceding discussions of the results by Kameoka, et al⁽¹⁵⁾, vessels with nozzle Types T13 and T*13 did not fail in the nozzles but in the longitudinal butt welds. There are a number of other literature references [including Reference (14)], in which longitudinal weld failures have occurred prior to failure of a nozzle in a vessel undergoing a cyclic pressure test.

B31.7 gives stress indices for longitudinal butt welds in straight pipe. For Class I piping with surfaces "as welded", these are: $C_1 = 1.1$, $K_1 = 1.2$. However, there is an important restriction to the K_1 -index; i.e., it is only applicable to pipe with a circular cross section. Unfortunately, Reference (15) does not give any significant details as to the longitudinal butt welds or the out-of-roundness of the vessel. Table 10 gives an evaluation of the tests under three separate assumptions:

- (1) The vessel cross section was circular, $C_1 = 1.1$, $K_1 = 1.2$
- (2) The vessel cross section was out-of-round such that

$D_{\max} - D_{\min} = 0.5t$. The equation shown in Footnote (1), Table D-201 of B31.7 was used to determine the additional stress due to out-of-roundness. The value of C_1 is still 1.1, but*

$$K_1 = 1.2 \left\{ 1 + \frac{0.5t}{t} \left[\frac{1.5}{1 + 0.455 \left(\frac{D_o}{t} \right)^3 \frac{P_o}{E}} \right] \right\} \quad (13)$$

* The procedure is that proposed in Reference (21) rather than that given in B31.7.

TABLE 10. EVALUATION OF CYCLIC PRESSURE TESTS ON LONGITUDINAL BUTT WELDS
IN CYLINDRICAL PRESSURE VESSELS, DATA FROM REFERENCE (15)

Model No.	P_o	$\frac{P_o D_o}{2t}$	S_n	$\frac{S_n}{3S_m}$	K_e	Test N_t	Assumed Cross Section (a)	S_p	$\frac{K_e S_p}{2}$	B31.7 N_c	$\frac{N_t}{N_c}$
T13-F	6,260	77,600	85,400	1.07	1.28	5,982	Circle	102,400	65,500	1,900	3.1
							Ellipse	139,000	89,000	850	7.0
							Limit	486,000	312,000	38	157.0
-D	5,550	68,800	75,700	0.95	1.00	9,102	Circle	90,800	45,400	6,000	1.5
							Ellipse	125,000	62,500	2,100	4.3
							Limit	431,000	215,000	90	101.0
-C	5,120	63,500	69,800	0.87	1.00	28,286	Circle	83,800	41,900	7,500	3.8
							Ellipse	117,000	58,500	2,750	10.3
							Limit	398,000	199,000	105	269.0
T*13-4	7,100	88,200	97,000	1.21	1.84	4,360	Circle	116,400	107,700	550	7.9
							Ellipse	155,000	143,000	240	18.2
							Limit	552,000	508,000	13	335.0
-2	5,690	70,500	77,600	0.97	1.00	9,502	Circle	93,100	46,600	5,000	1.9
							Ellipse	128,000	64,000	2,000	4.5
							Limit	443,000	221,000	85	112.0
-3	5,000	61,700	67,900	0.85	1.00	9,116	Circle	81,400	40,700	7,500	1.2
							Ellipse	114,000	57,000	3,000	3.0
							Limit	386,000	193,000	115	79.0
-1	4,270	52,900	58,200	0.73	1.00	21,135	Circle	69,800	34,900	13,000	1.6
							Ellipse	99,600	49,800	4,500	4.7
							Limit	332,000	166,000	160	132.0

(a) For elliptical cross section, $D_{max} - D_{min} = 0.5t$.

"Limit" calculation is based on Appendix A, Par. 1(c) of Reference (21).

The modulus of elasticity, E, was taken as 3×10^7 and $D_o/t = 22.7$ for the vessels, from which

$$K_1 = 1.2 + \frac{0.9}{1 + 0.000177 P_o}$$

- (3) The peak stress index was obtained by Appendix A, Paragraph 1 (c) of Reference (21). This method is applicable for any cross sectional shape with $D_{\max} - D_{\min} \leq 0.08 D_o$. It is based on limits to elastic strains considering maximum strain hardening and re-rounding under internal pressure, and is being considered for adoption by B31.7. The peak stress index is given by:

$$K_1 = (K_1)_{\text{round}} \left[1 + \frac{MS_y}{PD_o/2t} \right] \quad (14)$$

where, M = 2.0 for ferritic steels
 S_y = yield strength at design temperature
 (from Table A.3 of B31.7)
 P = design pressure .

Assuming $PD_o/2t = S_m$, then for A302 B at room temperature:

$$K_1 = 1.2 \left[\frac{2 \times 50,000}{26,700} \right] = 5.70$$

The material used in the vessel (see Table 8) has tensile properties similar to ASTM A302B; hence, the values of S_m , S_y , m, and n for A302B were used in the evaluation shown in Table 10.

The last column of Table 10 shows N_t/N_c values approaching unity if the vessels were actually round and had high-quality welds. However, even a small amount of assumed out-of-roundness brings N_t/N_c up significantly. The vessels were apparently formed in halves with two longitudinal butt welds. The abutting plate edges, particularly in experimental models, often are not rolled to the same radius as the body of the plate, leaving either a "peak" or a "flat spot" at the weld. For a given amount of out-of-roundness, these kinds of local irregularities give higher stresses than indicated by Equation (13) which is for an elliptical out-of-round shape. The "limit" analysis is applicable to any cross section shape (up to an out-of-roundness of $0.08 D_o$, which the

model vessel shells presumably met) and, as shown in Table 10, this analysis gives N_t/N_c values well above 20.

The purpose of including the data on longitudinal butt welds is to point out that such welds, in conjunction with out-of-roundness, can be a significant source of high stresses; a source recognized in B31.7. However, to bring the test results into perspective, it should be noted that the lowest number of cycles was 4360; this for a pressure range of zero to 7100 psi. The design pressure for this cylinder (of A302B, $S_m = 26,700$ psi) is about 2300 psi.

THERMAL GRADIENT LOADING

The third type of loading considered by B31.7 is that arising from thermal gradients. While a fair number of thermal fatigue tests on bar specimens are available in the literature, very little has been done on thermal cycling tests of piping components. Stewart and Schreitz⁽¹⁶⁾ give results of thermal shock tests on 6-inch Schedule 80 and Schedule 160 pipe and valves therein. Weisberg and Soldan⁽¹⁷⁾ give results of tests on pipe and girth-butt welds therein as do Tidball and Shrut⁽¹⁸⁾ and Gysel, Werner, and Gut⁽¹⁹⁾. These tests and results are not in sufficiently quantitative form to permit meaningful comparisons with the B31.7 fatigue approach. Further, these tests involve temperatures above that covered by B31.7 and therefore were not included in this study.

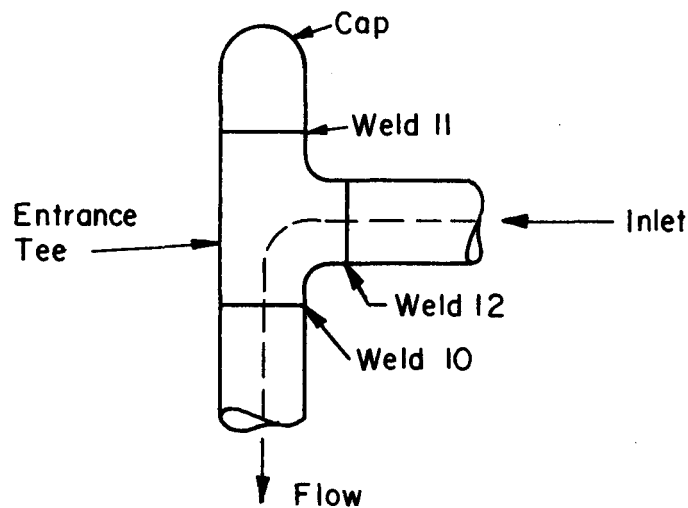
Recently, the writer obtained (from a source that cannot be referenced at this time) results of thermal gradient tests which are pertinent to this report. These tests, their results and a B31.7 evaluation of the results are discussed in the following.

Thermal gradient tests were conducted on a piping system made up of 1-inch Schedule 80 (1.315 inch O.D. x 0.179 inch nominal wall) piping and tees. The material was Ni-Cr-Fe Alloy 600. The fluid entrance to the section consisted of a butt-welding tee; the butt-welds between it and the pipe are the "components" of interest herein.

Thermal gradients were created by circulating hot water at $595 \text{ F} \pm 5 \text{ F}$ and $2900 \pm 100 \text{ psi}$ through the test section at the rate of 35 gpm, followed by circulating cold water at $70 \pm 10 \text{ F}$ and $60 \pm 10 \text{ psi}$. A typical thermal cycle was initiated by circulating hot water through the test section for 2 minutes; the fluid temperature near the inlet increasing from 70 F to 595 F in 2 seconds. Circulation of water was then stopped and the test section was allowed to "soak" at high temperature for 1.5 minutes in order to thoroughly heat the entire test section. During this period, the fluid temperature decreased 100 F. Cold water was then circulated through the test section for 3.5 minutes; the fluid temperature near the inlet decreasing from about 470 F to 70 F in 2 seconds. The total length of time for a complete cycle was 7 minutes.

At the completion of 2206 cycles, the test section was hydrostatically tested at a pressure of 4750 psi at 80 F for 15 minutes. There was no indication of leakage. A liquid penetrant inspection of the outside surface after the hydrostatic test did not indicate any cracks. The inlet tee and girth-butt welds between it and the pipe were then cut out of the test section and sectioned for internal surface inspection. The tee, flow direction, and welds are identified in the following sketch. Liquid penetrant inspection of

ORNL-DWG 71-12535



the inside indicated a crack in the heat-affected zone of weld Number 10. Further examination of the crack indicated it was about 0.030-inch deep (17 percent of the wall thickness) and had propagated in both a transgranular and intergranular pattern. The source of the test results was of the opinion that the crack pattern could have been caused by fatigue.

In summary, after 2206 cycles of thermal gradients, girth-butt weld Number 12 had no detectable cracks, girth-butt weld Number 10 had a small crack, the entrance tee had no detectable cracks. It is pertinent to note that girth-butt weld Number 12 would nominally undergo the highest thermal gradients; girth-butt weld Number 10 very slightly lower gradients and girth-butt weld Number 11, much lower thermal gradients. Details of the butt welds, or the relationship (if any) of the crack to root irregularities of weld Number 10 are not known at this time. The following B31.7-evaluation is based on the

assumption that girth-butt weld Number 10 was "as-welded", as classified in B31.7, Table D-201.

The value of S_n for the thermal gradient tests of girth-butt weld Number 10 is given by

$$S_n = \frac{P_o D_o}{C_1 2t} + \frac{1}{2(1-\nu)} E\alpha |\Delta T_1| \quad . \quad (15)$$

The M_i -term is not included in Equation (15) on the assumption that the test section was supported so that it was free to expand. The value of S_p is given by

$$S_p = K_1 C_1 \frac{P_o D_o}{2t} + \frac{K_3}{2(1-\nu)} E\alpha |\Delta T_1| + \frac{1}{1-\nu} E\alpha |\Delta T_2| \quad . \quad (16)$$

In the above equations

$$\left. \begin{array}{l} C_1 = 1.1 \\ K_1 = 1.2 \\ K_3 = 1.7 \end{array} \right\} \text{ per B 31.7 Table D-201 for "as welded" girth-butt weld}$$

$$P_o = \text{pressure range} = 2900 - 60 = 2840 \text{ psi}$$

$$D_o = \text{pipe O.D.} = 1.315 \text{ in.}$$

$$t = \text{pipe nominal wall thickness} = 0.179 \text{ in.}$$

$$\nu = \text{Poisson's ratio} = 0.3$$

$$E\alpha = \text{modulus times coefficient of thermal expansion} \\ = 226 \text{ for Ni-Cr-Fe Alloy 600 at } 70 \text{ F.}$$

The procedure for obtaining ΔT_1 and ΔT_2 is given in B31.7. The data given by Schneider⁽²²⁾ will be used as being sufficiently accurate. Specifically, for a step change in fluid temperature, Schneider's Chart 23 was used. This chart gives the temperature response of a plate insulated on one side after sudden exposure to a uniform temperature convective environment on the opposite side. The chart is given in terms of the parameters:

$$Bi = h\delta/K$$

$$Fo = \alpha_d \theta / \delta^2$$

where

$$h = \text{film coefficient, Btu/hr-ft}^2 \text{ } ^\circ \text{F}$$

δ = plate thickness, ft

K = thermal conductivity of plate material, Btu/hr-ft-°F

α_d = thermal diffusivity of plate material, ft²/hr

θ = time, hrs.

For the 1-inch Schedule 40 pipe, $\delta = 0.179/12 = .0149$ ft, $K = \sim .15$. For the heat-up side of the cycle, the flow rate of 35 gpm leads to a value of h of about 2500 Btu/hr-ft² - °F. Accordingly: $Bi = 4.13$. Schneider's Chart 23 then can be used to construct the temperature variation through the wall of the pipe as shown in Figure 4. Values of ΔT_1 and ΔT_2 can be calculated from Figure 4 by use of the equations:

$$\bar{T} = \frac{1}{t} \int_{-t/2}^{t/2} T(y) dy \quad (17)$$

$$\Delta T_1 = \frac{12}{t^2} \int_{-t/2}^{t/2} y T(y) dy \quad (18)$$

$$\Delta T_2 = \text{Max} (|T_o - \bar{T}| - |\Delta T_1|/2, |T_i - \bar{T}| - |\Delta T_1|/2, 0) \quad (19)$$

where T_o = outside surface temperature, °F; T_i = inside surface temperature, °F. Numerical integration was used to evaluate Equations (17) and (18); the results are shown in Figure 5 where ΔT_1 and ΔT_2 are plotted against time, θ . The maximums during the heat up side of the cycle are $\Delta T_1 = \sim .62 T_a$, $\Delta T_2 = \sim .23 T_a$.

Analysis of the cool-down side of the cycle would give graphs similar to Figures 5 and 6; with the sign of T_a reversed. The range of ΔT_1 and ΔT_2 during the cycle would be $.23 T_a$ and $.62 T_a$, where T_a is the sum of the step change in fluid temperature on the heat-up side of the cycle plus the step change on the cool-down side of the cycle. Nominally, T_a is equal to $2(595-70) = 1050$ °F. However, the "soak" period reduced the cool-down step change by 100 °F, and other effects may have reduced the effective T_a by another 100 °F. Accordingly, an estimate of $T_a = 800$ °F will be used; $|\Delta T_1| = 0.62 \times 800 = 496$ °F, and $|\Delta T_2| = 0.23 \times 800 = 184$ °F.

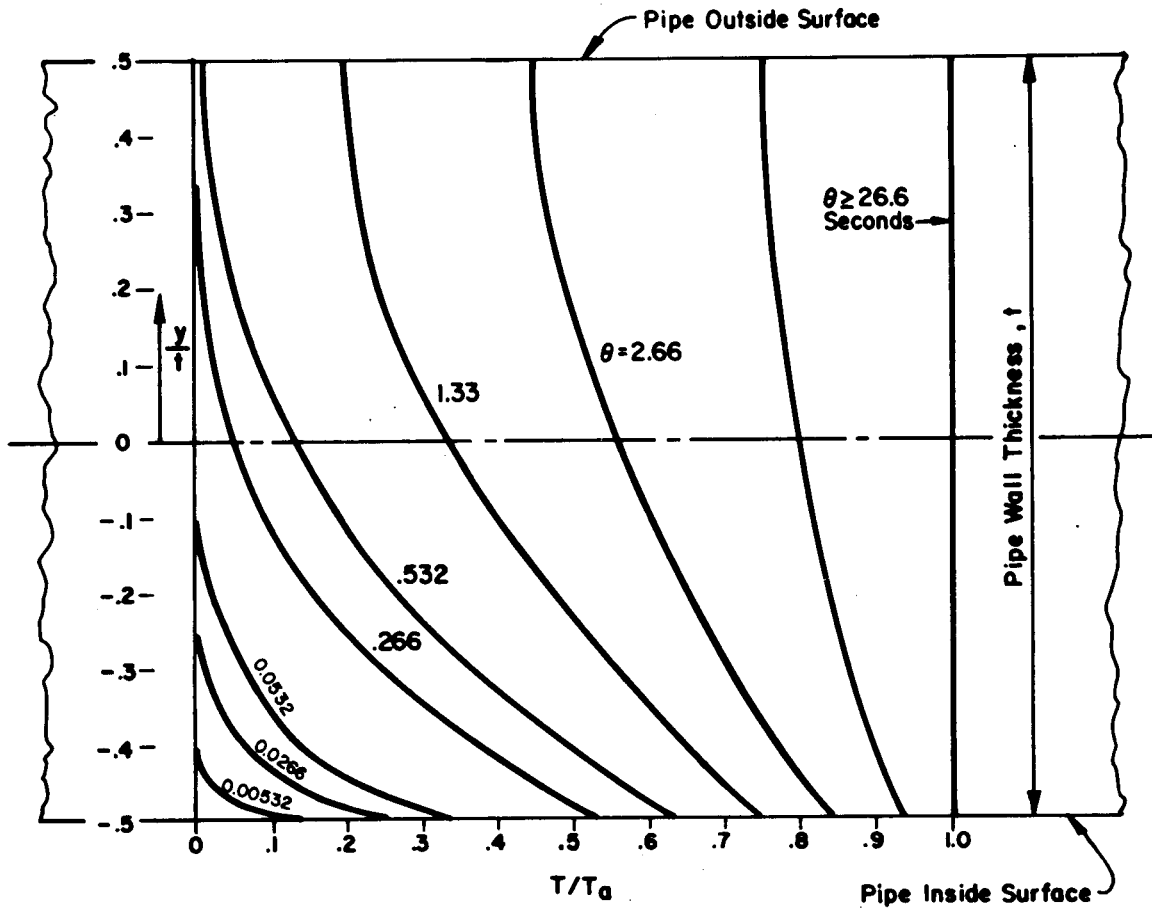
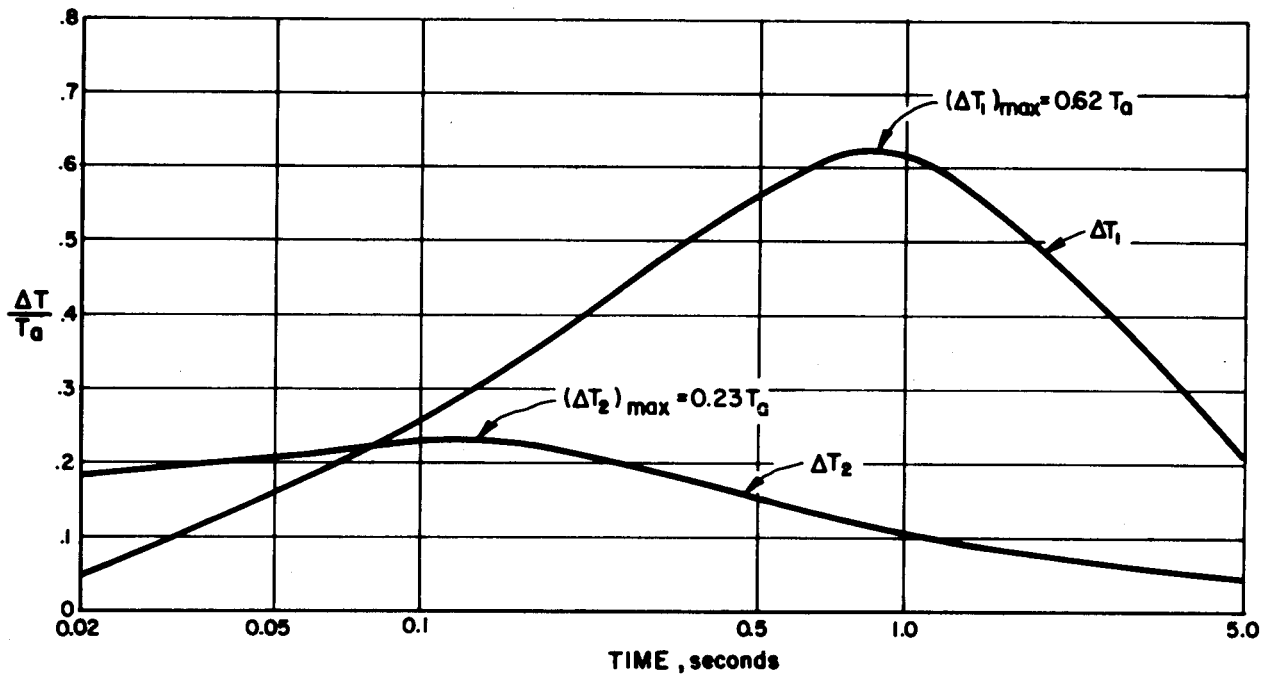


FIGURE 5. CALCULATED TEMPERATURE DISTRIBUTION THRU-WALL DURING HEATING PHASE, T_a = STEP CHANGE OF FLUID TEMPERATURE, $^{\circ}F$

ORNL-DWG 71-9093

FIGURE 6. CALCULATED ΔT_1 and ΔT_2 , HEATING PHASE, T_a = STEP CHANGE OF FLUID TEMPERATURE, °F

Equations (15) and (16) give

$$S_n = 1.1 \times \frac{2840 \times 1.315}{2 \times .179} + \frac{1}{1.4} \times 226 \times 496$$

$$= 11,475 + 80,070 = 91,545 \text{ psi,}$$

$$S_p = 1.2 \times 1.1 \times \frac{2840 \times 1.315}{2 \times .179} + \frac{1.7}{1.4} \times 226 \times 496 + \frac{1}{.7} \times 226 \times 184$$

$$= 13,770 + 136,110 + 59,400 = 209,280 \text{ psi.}$$

For Ni-Cr-Fe alloy 600 (SB163, annealed) at 600 F, $S_m = 23,300$ psi. The value of K_e , by Equation (3) herein,* is

$$K_e = 1 + 3.33 \left[\frac{91,545}{3 \times 23,300} - 1 \right], \quad 3.33 = 2.032$$

and, by Equation (4)

$$S_{alt} = \frac{2.032 \times 209,280}{2} = 212,630 \text{ psi}$$

From Figure 2, the calculated cycles, N_c , is 140. The ratio $N_t/N_c \geq 2200/140 = 16$. Accordingly, the indices method is conservative as compared to this single set of test data on thermal gradient loading; particularly considering that girth-butt weld Number 10 had a crack depth of only 17 percent of the wall thickness, and girth-butt weld Number 12 had no crack indications after 2200 thermal gradient cycles.

It is of some interest to note that if K_e were to be taken as unity, the $S_{alt} = 105,000$; $N_c = 1100$, $N_t/N_c \geq 2200/1100 = 2.0$.

While details of the geometry of the entrance tee are not known, calculations based on some rough assumptions lead to the conclusion that the indices method would give about the same value of N_c as obtained for the girth-butt weld. No cracks were found in the entrance tee after 2200 thermal gradient cycles.

* Values of m and n for Monel are the same as for austenitic stainless steel.

COMPARISONS WITH ANSI B31.1 (POWER PIPING)
FATIGUE DESIGN BASIS

A fatigue-based design analysis procedure for thermal expansion loading was introduced into the (then) ASA B31.1 Piping Code in 1955. The procedure is used, essentially as developed in 1955, in the present version of the ANSI (USAS) Power Piping Code, B31.1.0 - 1967⁽²³⁾ (hereinafter referred to as B31.1). The background of this design analysis involved a stress range concept and maximum shear stress as a fatigue criterion. It is of interest to compare this fatigue analysis, developed some 20 years ago, with the fatigue analysis represented by the B31.7 stress indices and ASME Code Case 1441.

Carbon Steel at Room Temperature

As a first step, it is pertinent to construct an adjusted S-N curve to represent the K_e -factor of ASME Code Case 1441, as shown in Figure 7. The "A-curve" in Figure 7 is taken from Figure 1 herein; it is the design cycle curve for carbon steel. The "B-curve" in Figure 7 represents the K_e -factor for the specific set of conditions: A106 Grade B carbon-steel material at room temperature ($S_m = 20,000$, $m = 3.0$, $n = 0.2$), $S_n = S_p$ (i.e., a component such as an elbow for which $K_2 = 1.0$). The B-curve is constructed as follows.

- (1) For a selected value of $S_n/3S_m > 1.0$, calculate K_e ; e.g.,

$$\frac{S_n}{3S_m} = 1.2, K_e = 1 + 2 \left[\left(\frac{S_n}{3S_m} \right) - 1 \right] = 1.4$$

- (2) Enter Figure 7 with $S_a = \frac{K_e S_p}{2} = \frac{K_e}{2} \frac{S_n}{3S_m} \times 60,000$

(Recall that $S_n = S_p$, and $3S_m = 60,000$)

e.g., enter at $S_a = \frac{1.4}{2} \times 60,000 = 50,400$

- (3) Proceed horizontally to intersection with A-curve, then downward to value of $S_n/2$. (Recall that S_n is a range, S_a an amplitude.) This establishes a point on the B-curve; e.g., for $S_n/3S_m = 1.2$, $S_a = 50,400$ gives $N = 3,900$; $S_n/2 =$

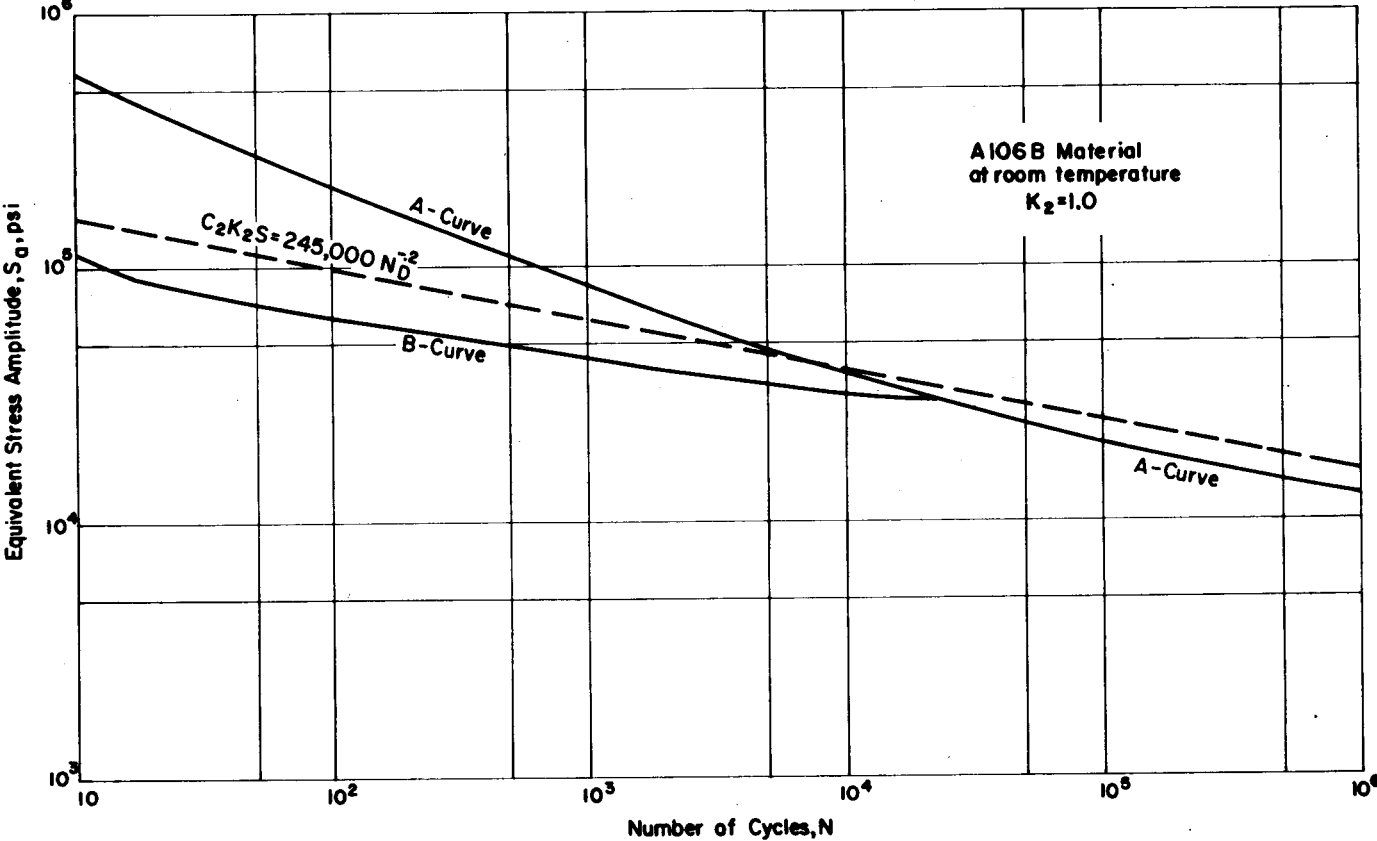


FIGURE 7. COMPARISON OF B31.7 INDICES/METHOD WITH B31.1 ANALYSIS BASIS, CARBON STEEL AT ROOM TEMPERATURE, $K_2 = 1.0$

$60,000 \times 1.2/2 = 36,000$; $N = 3,900$, $S_a = 36,000$ is a point on the B-curve.

- (4) Repeat Steps (1) through (3) with other values of $S_n/3S_m > 1.0$ to obtain other points on the B-curve.

The third line in Figure 7, labeled $C_2 K_2 S = 245,000 N_D^{-0.2}$, represents the basis of the B31.1 fatigue design procedure. It is derived from the general equation developed by Markl⁽⁴⁾:

$$iS = 245,000 N^{-0.2} \quad (20)$$

where $S = (M/Z)$, nominal stress amplitude

i = fatigue based stress intensification factor in relation to the fatigue strength of a "typical" girth-butt weld, for which $i = 1.0$

N = cycles-to-failure (through-the-wall-crack).

To compare Equation (20) with the B31.7 indices/method, two adjustments must be made, one with respect to the i -factor and one with respect to N .

The i -factor in Equation (20) is related to the fatigue strength of a "typical" girth-butt weld whereas the B31.7 S-N curve is based on polished bar data. The following points are pertinent to this relationship.

- (1) For butt-welding elbows, the elastic stress (as determined experimentally or theoretically) is essentially twice the i -factor for elbows as developed from fatigue tests on elbows and used in Equation (20).
- (2) Strain controlled fatigue data on polished bars, in the cycle range of 4×10^4 to 10^6 cycles (where K_e is 1.0), and on which the B31.7 fatigue analysis is based, is given approximately by

$$S = 490,000 N^{-0.2} \quad (21)$$

where S = equivalent stress amplitude

- (3) A few tests on branch connections in which the elastic stress was first determined by strain gages and later the specimens were subjected to fatigue tests, also indicate that the i -factor in Equation (20) represents about one-half of the actual elastic stress intensity (see Reference 24).

All three of the above points indicate that the effective stress intensification factor of a typical girth-butt weld, as related to strain controlled, polished bar fatigue data, is approximately two. Accordingly, Equation (20) should be written in the form

$$(2i) S = 490,000 N^{-.2} \quad . \quad (22)$$

The C_2 or C_2K_2 stress indices given in B31.7 are (with some subtle exceptions which will not be gone into here) equal to 2i as derived from fatigue tests.

Equation (22), however, is still a failure-prediction equation; i.e., N is the cycles-to-failure. The B-curve and lower end of the A-curve of Figure 7 represents a design curve which contains a factor of safety of about two on stress. Applying this factor of safety of two on stress to Equation (22) gives

$$(2i) S = 245,000 N_D^{-.2} \quad (23)$$

where N_D = design cycles, or in terms of B31.7 indices

$$C_2K_2 S = 245,000 N_D^{-.2} \quad . \quad (24)$$

While Equation (24) has the same constant as Equation (20), it has an entirely different meaning.

Comparison of Equation (24) with the B-curve and lower portion of the A-curve on Figure 7 is, therefore, a direct comparison of the B31.7 indices method with the B31.1 basis. It will be noted that both analysis have about the same overall slope and that the B31.7 indices method is conservative with respect to Equation (24) for N_D from 10 to 10^6 . If Equation (24), with its associated C_2 -indices for butt-welding elbows and butt-welding tees, is a good representation of the fatigue life of such components then we would expect the B31.7 indices method to be conservative, particularly in the range of 10^2 to 10^4 cycles. Examination of the data in Tables 2 and 3 confirm this hypothesis; i.e., values of N_t/N_c are obtained for carbon-steel butt-welding elbows and butt-welding tees of from 55 to > 2600 .

The preceding discussion has been concerned with components where K_2 is 1.0. It is appropriate now to consider the effect of K_2 greater than 1.0. The simplest example is the "as-welded" girth-butt weld for which $C_2 = 1.0$, $K_2 = 1.8$. Figure 8 is analogous to Figure 7 except now the value of S_a is more specifically considered as the "total stress", the value of $S_n/2$ is

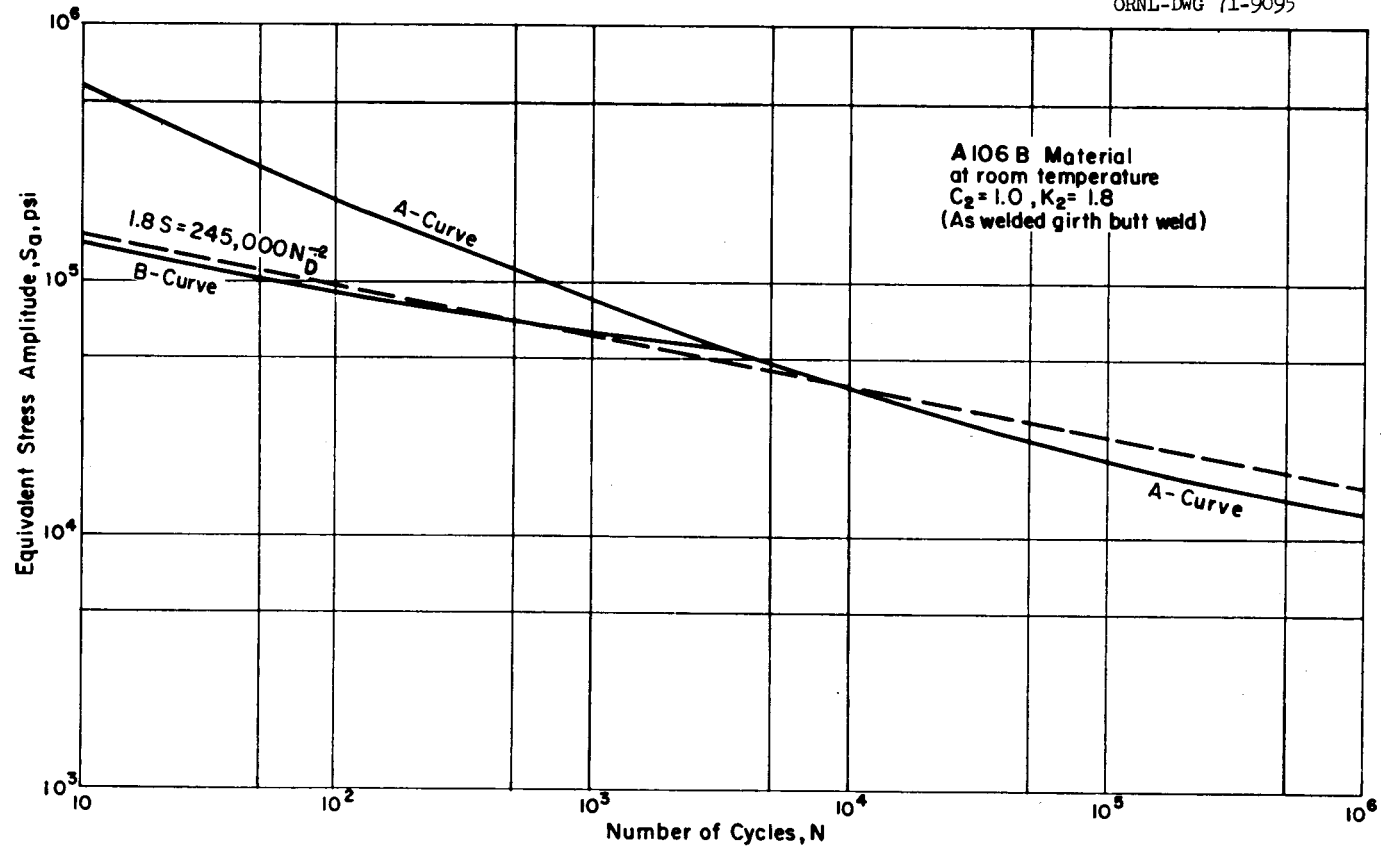


FIGURE 8. COMPARISON OF B31.7 INDICES/METHOD WITH B31.1 ANALYSIS BASIS, CARBON STEEL AT ROOM TEMPERATURE, $C_2 = 1.0, K_2 = 1.8$, AS-WELDED GIRTH-BUTT WELD

(1/1.8) times the total stress. Accordingly, the B-curve resulting from the K_e -factor starts at $S_a = 1.8 \times 30,000 = 50,400$ psi. Figure 8 indicates almost an exact agreement between Equation (24) for girth-butt welds (with $C_2 = 1.0$, $K_2 = 1.8$) and the B31.7 indices method for design cycles between 10 and 20,000. Here, if Equation (24) is a good representation of the fatigue life of girth-welded joints, we would expect a lesser degree of conservatism than obtained for butt-welding elbows or butt-welding tees. Examination of N_t/N_c values given in Table 1 indicate that this is indeed the case for carbon steel girth-butt welds for which the range of N_t/N_c is between 13 and 18 whereas for carbon steel butt-welding elbows and butt-welding tees the range of N_t/N_c is between 55 and > 2600 .

Carbon Steel at Elevated Temperatures

The B31.1 fatigue analysis procedure introduces a temperature effect through the use of the allowable expansion-stress parameter

$$S_A = 1.25 S_c + 0.25 S_h \quad (25)$$

where S_c = basic allowable stress at minimum (cold) temperature

S_h = basic allowable stress at maximum (hot) temperature.*

The B31.7 indices method introduces temperature effect only through the calculation of K_e . Code Case 1441 does not explicitly state at what temperature S_m is to be taken; other places in both B31.7 and ASME Section III suggest that it should be taken at the mean of the maximum and minimum temperature associated with the stress cycle. (See Footnote 1 to Table F-104 in B31.7 or Footnote 1 to Table N-414 in ASME Section III). Under this interpretation, if we now consider a minimum temperature of 100 F, maximum temperature of 700 F, mean temperature of 400 F, for A106 Grade B the value of S_m at 400 F is the same as at 100 F, hence there is no temperature effect under the B31.7 indices method. The B31.1 procedure, for the same materials and temperatures, would introduce a very small temperature effect; i.e.,

* Under certain conditions [See B31.1, 102.3.2(d)] the coefficient of S_h may be greater than 0.25 and may be as large as 1.25.

$$\text{At } T_c = T_h = 100 \text{ F; } 1.25 S_c + 0.25 S_h = 22,500$$

$$\text{At } T_c = 100 \text{ F; } T_h = 700 \text{ F; } 1.25 S_c + 0.25 S_h = 22,338 \quad .$$

Accordingly, the B31.7 indices method and B31.1 procedure agree that the fatigue life of A106 B carbon steel is essentially independent of temperature in a stress cycle associated with a temperature change from 100 F to 700 F.

Austenitic Stainless Steel at Room Temperature

Figure 9 gives comparisons analogous to those shown for A106 B carbon steel by Figure 7, except Figure 9 is for A312 TP304 stainless steel. The A-curve, taken from Figure 2, is the design cycle curve for austenitic stainless steels. The B-curve represents the K_e -factor for the specific set of conditions: A312 TP304 at room temperature ($S_m = 20,000$, $m = 1.7$, $n^* = 0.3$), $S_n = S_p$ (i.e., a component such as an elbow for which $K_2 = 1.0$). The B-curve is constructed in a manner analogous to that described previously.

The curve marked

$$C_2 K_2 S = 281,000 N_D^{-.2} \quad (26)$$

is derived in the same way as Equation (24), except that it now has a constant of 281,000 as suggested by Markl⁽²⁰⁾ for austenitic stainless steel at room temperature. If Equation (26), with its associated C_2 -indices for butt-welding elbows and butt-welding tees, is a good representation of the fatigue life of such components, then we would expect the B31.7 indices method to be conservative, particularly in the range of 10^2 to 10^4 cycles. Examination of the data for austenitic stainless steel tested at room temperature shown in Tables 2 and 3 indicates that this is so; the values of N_t/N_c (3 elbows, 5 tees) range from 45 to 660 with an average of 320.

Figure 9 indicates that, if Equation (26) is "correct", then the B31.7 indices method is unconservative for values of N_D above 10^5 . While a "knee" and an "endurance strength" exists for fatigue tests of polished bars,

* The value of $n = 0.3$ is taken from proposed changes in Code Case 1441. A comparison of $n = 0.5$ (in 1441) with $n = 0.3$ is shown in Appendix A.

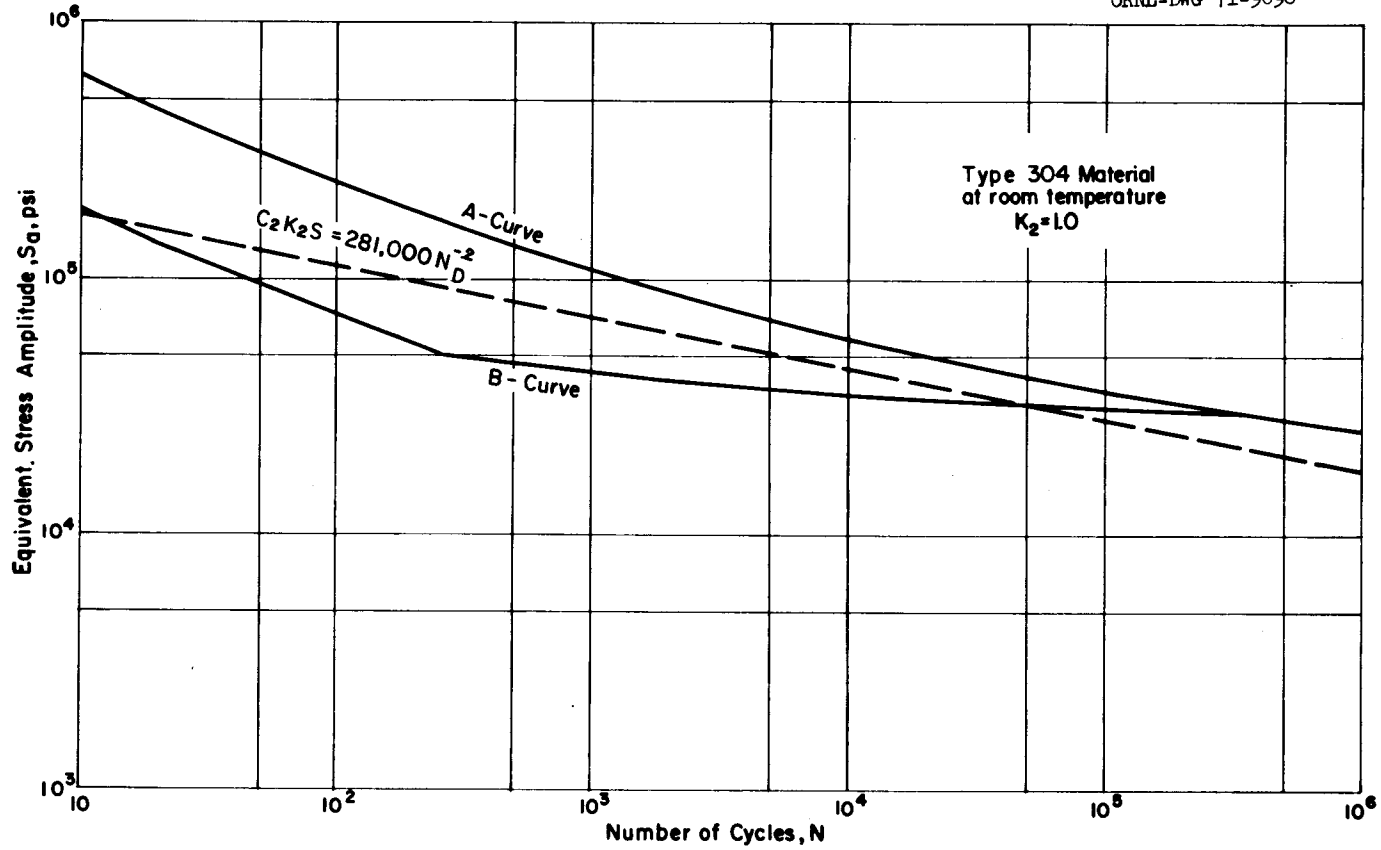


FIGURE 9. COMPARISON OF B31.7 INDICES/METHOD WITH B31.1 ANALYSIS BASIS, TP 304 STAINLESS STEEL AT ROOM TEMPERATURE, $K_2 = 1.0$

whether an "endurance strength" exists for piping components is perhaps open to question. Equation (26) indicates there is neither a knee nor an endurance strength; the B31.7 indices method does assume an endurance strength. The question, for typical piping system design, would seem to be only of academic interest unless severe vibration exists in the piping system.

Figure 10 gives comparisons for an "as-welded" girth-butt weld in a TP312 stainless-steel pipe, analogous to Figure 8 for A106 Gr.B carbon steel. Figure 10 indicates almost an exact agreement between Equation (26) for girth-butt welds (with $C_2 = 1.0$, $K_2 = 1.8$) and the B31.7 indices method for cycles between 10 and 1,000, with the B31.7 indices method becoming relatively less conservative at higher cycles.

Austenitic Stainless Steel at Elevated Temperatures

For Type 304 stainless steel with a cycle from 100 F to 800 F, the B31.1 fatigue analysis procedure would contain a temperature effect as indicated by:

$$\text{At } T_c = T_h = 100 \text{ F; } 1.25 S_c + 0.25 S_h = 28,125 \text{ psi}$$

$$\text{At } T_c = 100, T_h = 800 \text{ F; } 1.25 S_c + 0.25 S_h = 26,000 \text{ psi} \quad .$$

If Code Case 1441 is interpreted as implying that S_m is to be taken at the mean temperature of the cycle, which in this case would be at $T = 450$ F, then $S_m = 17,000$ is used for calculating K_e rather than $S_m = 20,000$ for room temperature.

Figure 11 consists of a reproduction of Figure 9, with super-position of the S-N curves for temperature. For the B31.1 basis, the constant of 281,000 is multiplied by 26,000/28,125. For the B31.7 indices/method, the correction is through the K_e -factor. It is apparent that the temperature effect by the two approaches is about the same, however, the B31.1 approach applies for all values of N_D ; the B31.7 approach only for 260 to 10^6 cycles. (No correction appears at low cycles because K_e carries an upper bound of $1/n$.)

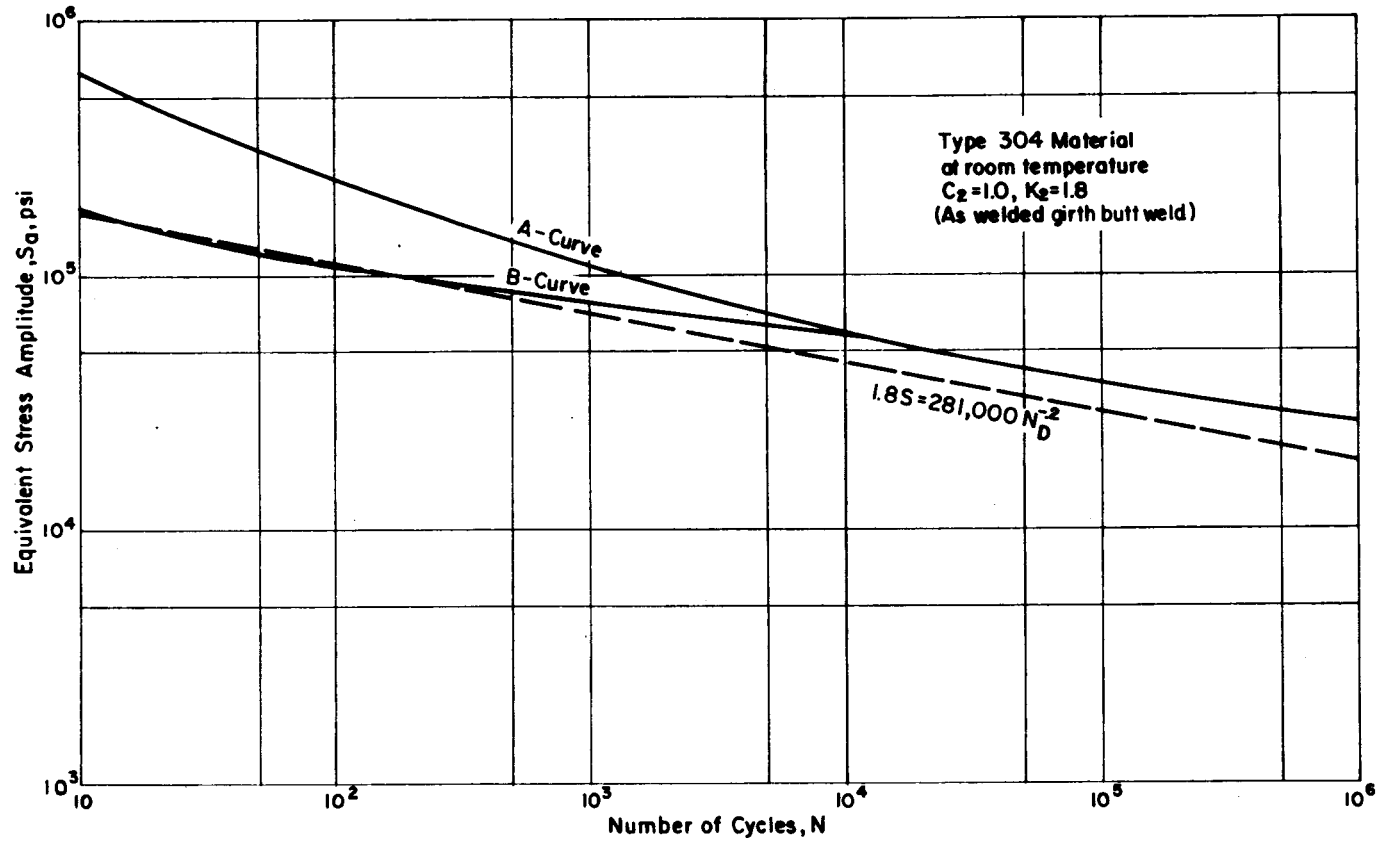


FIGURE 10. COMPARISON OF B31.7 INDICES METHOD WITH B31.1 ANALYSIS BASIS,
 TP 304 STAINLESS STEEL AT ROOM TEMPERATURE, $C_2 = 1.0$, $K_2 = 1.8$,
 AS-WELDED GIRTH-BUTT WELD

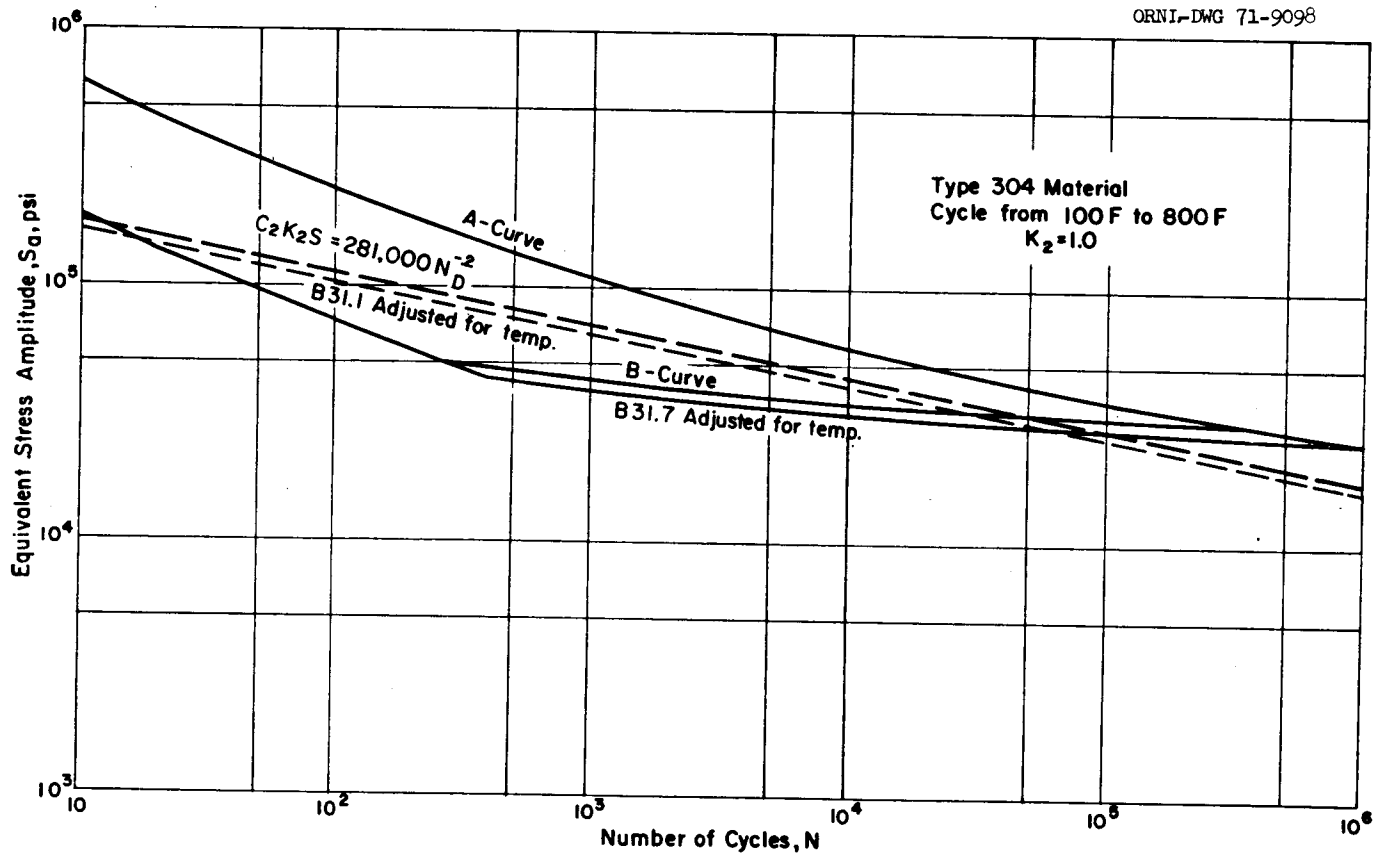


FIGURE 11. EFFECT OF TEMPERATURE, TYPE 304 STAINLESS STEEL

Permissible Design Cycles

In the preceding discussion, comparisons have been made between the basis for the B31.1 fatigue design procedure and the B31.7 indices method. However, the actual relation between stresses due to moment loading (restraint of thermal expansion) and permissible design cycles in B31.1 is given by Table 102.3.2(c) in B31.1.

Number of Equivalent Full Temperature Cycles*	f
7000 and less	1.0
7000 to 14,000	0.9
14,000 to 22,000	0.8
22,000 to 45,000	0.7
45,000 to 100,000	0.6
100,000 to over	0.5

* B31.1, like B31.7, uses Minor's cumulative damage hypothesis for summing of cycles of different magnitude.

Where f is defined as the "stress range reduction factor" and is used in the equation:

$$S_A = f[1.25 S_c + 0.25 S_h + (S_h - S_\ell)] \quad (27)$$

where

S_A = allowable stress range for expansion stresses
 S_c = basic allowable stress at minimum (cold) temperature
 S_h = basic allowable stress at maximum (hot) temperature
 S_ℓ = sum of longitudinal stresses due to pressure, weight,
and other sustained loads.

Figure 12 shows comparisons between Equation (27) and the B31.7 indices method for the following specific conditions.

- (1) The material is A106 Grade B.
- (2) The temperature extremes of the cycle are 100 F and 700 F.
 S_m in the B31.7 procedure is taken as 20,000 psi at 400 F.
- (3) In the B31.7 procedure, the life usage factor for cyclic pressure and cyclic temperature gradients are assumed to be negligible.

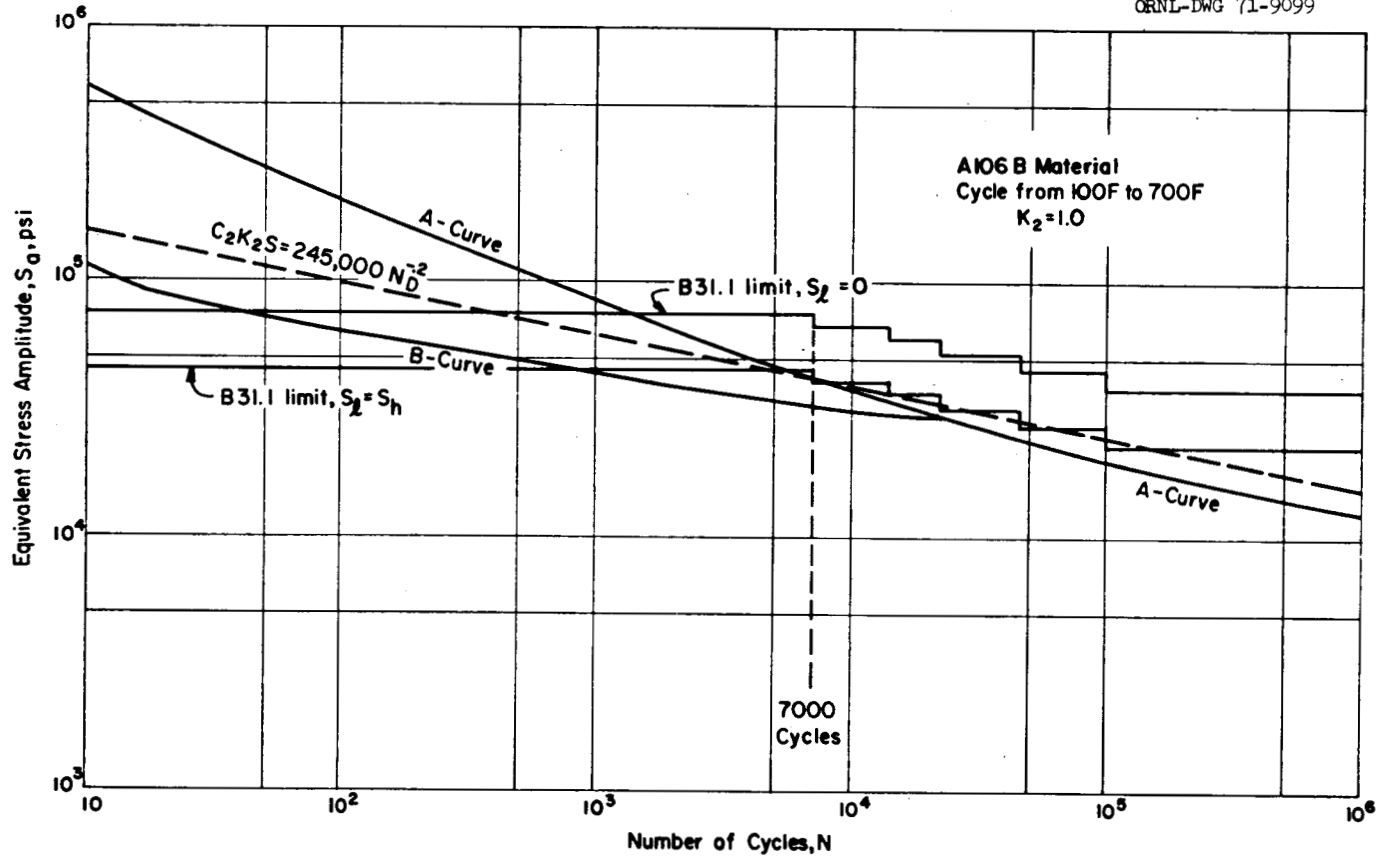


FIGURE 12. COMPARISON OF B31.1 PERMISSIBLE DESIGN CYCLES WITH B31.7 INDICES METHOD
A106 B MATERIAL IN CYCLE FROM 100F TO 700F

- (4) In the B31.7 procedure, the K_2 -index is assumed to be unity.
- (5) In the B31.1 procedure, two assumptions are made concerning the value of S_ℓ , and two corresponding B31.1 curves are shown in Figure 12; these are:

(a) $S_\ell = S_h$

(b) $S_\ell = 0$.

It can be seen in Figure 12, for $S_\ell = S_h$, that the step changes represented by Equation (27) are a good approximation of the "basic curve", $C_2 K_2 S = 245,000 N^{-.2}$, between 5,000 and 200,000 cycles. Use of the allowable stress at 7,000 cycles for all cycles less than 7,000 is not supported by any test data, in-so-far as the writer is aware, and presumably represents an arbitrary code committee decision for simplification of the code rules. Similarly, use of the allowable stress at 100,000 cycles for all cycles greater than 100,000 is presumably an arbitrary code decision. This implies that there is a "knee" in the S-N curve and that the endurance strength (considering the factor-of-safety of two in Figure 12) is about 45,000 psi. For an actual application of cycles far in excess of 100,000, the B31.1 approach may be unconservative; occurrence of such a large number of cycles in a piping system would probably result only from vibration. Vibration, per se, is not covered by the B31.1 analysis.

For $S_\ell = 0$, Figure 12 shows that the B31.1 S-N curve is shifted upward by the ratio of $(1.25 S_c + 1.25 S_h) / (1.25 S_c + 0.25 S_h)$. This appears to be an unconservative approach because the basic data was obtained almost entirely with $S_\ell = 0$. A more reasonable approach would be to make the $S_\ell = 0$ curve an approximation of the basic data and then to shift the $S_\ell = S_h$ curve downward. It can be seen in Figure 12 that the $S_\ell = S_h$ curve is unconservative for higher cycles both with respect to the basic B31.1 data and the B31.7 indices method.

Figure 13, for type 304 stainless steel, is based on the same set of conditions as Figure 12, except that the temperature extremes are 100 F and 800 F; S_m is taken as 17,000 psi at 450 F. Similar observations for stainless steel can be made from Figure 13 as were made for carbon steel with Figure 12.

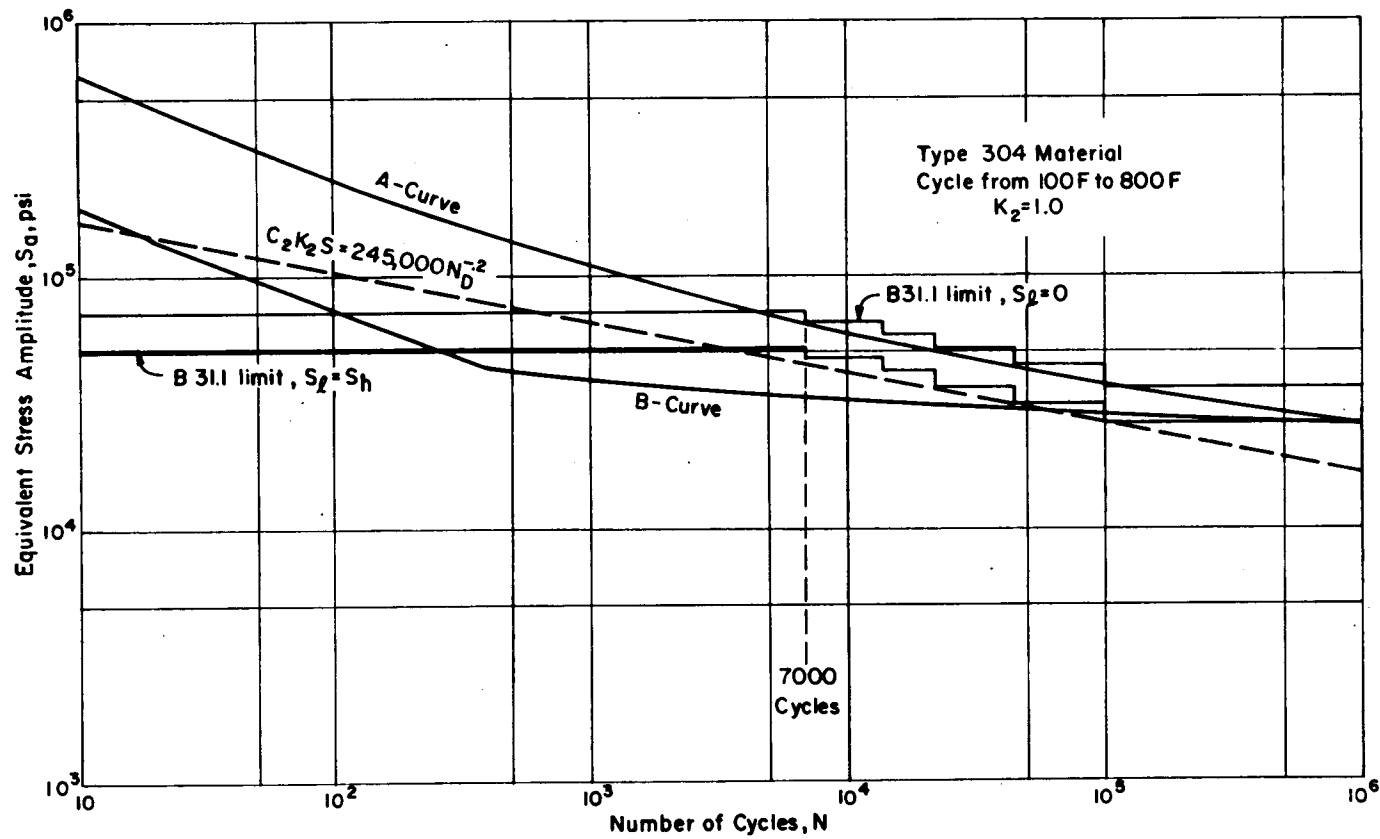


FIGURE 13. COMPARISON OF B31.1 PERMISSIBLE DESIGN CYCLES WITH B31.7 INDICES METHOD, TYPE 304 MATERIAL IN CYCLE FROM 100F TO 800F

SUMMARY

Comparisons between the B31.7 indices/Code Case 1441 fatigue analysis method and fatigue test data on several types of piping components indicate that, with the possible exception of girth butt welds in austenitic stainless steel pipe subjected to moment loading at elevated temperatures, the B31.7 indices in conjunction with Case 1441 analysis method provides a conservative procedure for determining an acceptable design fatigue life when $S_n > 3S_m$. The criterion upon which this conclusion is based is that, on the average, the value of N_t/N_c should be equal to or greater than 20. (N_t = cycles to failure as defined by a thru-the-wall crack; N_c = calculated design cycles using the B31.7 indices/Case 1441 method.)

The single available test of a girth butt weld in 304 stainless steel pipe with cyclic moment loading at 550 F (specimen HW-3A in Table 1) gave $N_t/N_c = 6.3$. Additional tests of this component at elevated temperatures is suggested (see discussion on p. 12).

Girth butt welds in carbon steel pipe under cyclic moment loading gave N_t/N_c from 13 to 18. This is somewhat on the low side of the criterion of $N_t/N_c \geq 20$; the available margin seems adequate but certainly not over-conservative.

All other components with moment loading (butt welding elbows, butt welding tees, fabricated tees, drawn outlet tees, girth fillet welds and notched pipe) gave N_t/N_c values which, on the average, were well above 20.

Cyclic internal pressure tests of nozzles in cylindrical pressure vessels gave N_t/N_c from 10.4 to > 860 . Most of these tests involved

maximum pressures such that the nominal hoop stress significantly exceeds the primary stress limit for pressure loading. There is some suggestion that the K_e -factor over-compensates for $S_n > 3S_m$; i.e., in general the high values of N_t/N_c were obtained for $S_n \gg 3S_m$, the low values for $S_n = \sim 3S_m$.

Results of cyclic pressure tests on longitudinal welds are presented. While some comparisons are made, significant details of the welds are not available; the data were included to draw attention to this potential "weak zone" in pressure vessels and piping.

Results of the one available cyclic thermal gradient test gave $N_t/N_c \geq 16$ for a girth butt weld in 2" Sch. 80 Monel pipe.

As remarked in the introduction, no implication is intended that the test data are sufficiently broad in scope to confirm the validity of the indices method for all combinations of piping components, materials, temperatures and loadings. In particular, test data with combinations of cyclic loadings are lacking. A test of a butt welding elbow or butt welding tee with combined cyclic moment and cyclic internal pressure would contribute significantly towards determining if combined loadings are worse than expected from the sum of the effects of the separate loadings.

Comparisons with the B31.1 fatigue design basis and the B31.7 indices/Case 1441 method indicate a gratifying degree of agreement between these two methods of analysis, considering that the B31.1 basis was developed some 20 years prior to Code Case 1441 and that the latter was developed following an entirely different approach to the problem of fatigue analysis for loadings at which $S_n > 3S_m$.

REFERENCES

- (1) ASME Boiler and Pressure Vessel Code, Section III, Nuclear Vessels, 1968, and Criteria of Section III of the ASME Boiler and Pressure Vessel Code for Nuclear Vessels (1964). Published by the American Society of Mechanical Engineers, 345 E. 47th Street, New York, N.Y. 10017.
- (2) USA Standard Code for Pressure Piping, Nuclear Power Piping, USAS B31.7-1969. Published by the American Society of Mechanical Engineers, 345 E. 47th Street, New York, N.Y. 10017.
- (3) Rodabaugh, E. C., "Comparison of USAS B31.7 Plastic Fatigue Analysis With Test Data on Piping Components", Phase Report 115-2, February, 1969. Report to Applied Mechanics Section, Reactor Division, Oak Ridge National Laboratory.
- (4) Markl, A.R.C., "Fatigue Tests of Piping Components", Trans. ASME, Vol. 74, pp. 287-303 (1952).
- (5) Markl, A.R.C., "Fatigue Tests of Welding Elbows and Comparable Double-Mitre Bends", Trans. ASME, Vol. 69, pp. 869-879 (1947).
- (6) Grigory, S. C., "Studies of the Fatigue Strength of Pressure Vessels, Fatigue Tests of One-Half Scale Model Pressure Vessels", April 29, 1968, Southwest Research Institute, San Antonio, Texas, to USAEC.
- (7) Markl, A.R.C., and George, H. H., "Fatigue Tests on Flanged Assemblies", Trans. ASME, Vol. 72, pp. 77-87 (1950).
- (8) Kiss, E., Heald, J. D., and Hale, D. A., "Low-Cycle Fatigue of Prototype Piping", General Electric (San Jose) Report GEAP-10135, January, 1970.
- (9) Greenstreet, W. L., Moore, S. E., and Callahan, J. P., "1970 Annual Progress Report on Studies in Applied Solid Mechanics (Nozzles and Piping Components)", Oak Ridge National Laboratory, to be published.
- (10) Newman, R. P., "The Influence of Weld Faults on Fatigue Strength With Reference to Butt Joints in Pipe Lines", Trans. Institute of Marine Engineers, Vol. 68, p. 153 (1956).
- (11) O'Toole, W. G. and Rodabaugh, E. C., "Fatigue Tests on 4" Std. Wt. Carbon and Stainless-Steel Pipe and Circumferential Butt-Weld Joints", Tube Turns, Louisville, Ky., Report No. 8.031, October, 1961.
- (12) Meister, R. P., et al., "Effects of Weld-Joint Imperfections on Piping Performance", Battelle Memorial Institute, Columbus, Ohio, October 30, 1964.

"Effects of Multiple-Weld Repairs and 400 F Interpass Temperature on Piping Performance", Battelle Memorial Institute, Columbus, Ohio, October 30, 1964.

- (13) Dawes, M. G., "Fatigue Strength of Tubes Butt-Welded Using a Ceramic Coated Backing Member", British Welding Journal, p. 304, June, 1967.
- (14) Pickett, A. G. and Grigory, S. C., "Studies of the Fatigue Strength of Pressure Vessels, Part 1. Cyclic Pressure Tests of Full-Size Pressure Vessels", September, 1966, Southwest Research Institute, San Antonio, Texas, to USAEC.
- (15) Kameoka, T., Sato, E., An, B., and Sato, Y., "Low-Cycle Fatigue of Pressure Vessels with Butt-Welded Nozzles", Proceedings of First International Conference on Pressure Vessel Technology, Delft, 1969, Available from ASME, 345 E. 47th Street, New York, N. Y.
- (16) Stewart, W. C. and Schreitz, W. G., "Thermal Shock and Other Comparison Tests of Austenitic and Ferritic Steels for Main Steam Piping", Trans. ASME, Vol. 72, pp. 1051-1072 (1950).

Stewart, W. C. and Schreitz, W. G., "Thermal Shock and Other Comparison Tests of Austenitic and Ferritic Steels for Main Steam Piping - A Summary Report", Trans. ASME, Vol. 75, pp. 1051-1072 (1953).
- (17) Weisberg, H. and Soldan, H. M., "Cyclic Heating Test of Main Steam Piping Materials and Welds at the Searin Generating Station", Trans. ASME, Vol. 76, pp. 1085-1091 (1954).
- (18) Tidball, R. A. and Shrut, M. M., "Thermal-Shocking Austenitic Stainless Steels with Molten Metals", Trans. ASME, Vol. 76, pp. 639-643 (1954).
- (19) Gysel, W., Werner, A., and Gut, K., "Thermal Shock Behavior of Various Grades of Cast Steel", Proceedings of Joint International Conference on Creep, Institute of Mechanical Engineers, London, pp. 3-33 to 3-41 (1963).
- (20) Markl, A. R.C., Discussion of Reference (16), Trans. ASME, Vol. 75, p. 1,068 (1953).
- (21) Rodabaugh, E. C., "Stresses in Out-of-Round Pipe Due to Internal Pressure, ORNL-TM-3244, January, 1971.
- (22) Schneider, P. J., "Temperature Response Charts", John Wiley & Sons, 1963.
- (23) USA Standard Code for Pressure Piping, Power Piping, USAS B31.1.0-1967 Published by the American Society of Mechanical Engineers, 345 E. 47th Street, New York, N.Y. 10017.
- (24) Rodabaugh & Atterbury, "Stresses at Nozzles in Cylindrical Shells Loaded with Pressure, Moment or Thrust: Phase Report 5 of Evaluation of Theoretical and Experimental Data on Radial Nozzles in Pressure Vessels", TID-24342, U.S.A.E.C. Division of Technical Information.

APPENDIX A

ASME BOILER CODE CASE 1441 AND
POSSIBLE REVISIONS THEREOF

CASE 1441

INTERPRETATIONS OF ASME BOILER AND PRESSURE VESSEL CODE

Approved by Council, December 29, 1969

Case 1441
(Special Ruling)
Waiving of $3Sm$ limit for Section III
Construction

Inquiry: The purpose of the $3Sm$ limit on the range of primary-plus-secondary stress (N-414.4) is to assure validity of the S_a value used in the fatigue evaluation. What modification may be made in the fatigue evaluation which will permit waiving the $3Sm$ limit?

Reply: It is the opinion of the Committee that the $3Sm$ limit on the range of primary-plus-secondary stress (N-414.4) may be waived if:

(1) There are not more than 1000 cycles of primary plus secondary stress range greater than $3Sm$.

(2) The value of S_a used for entering the design fatigue curve is increased by the factor K_e .

Where:

$$K_e = 1.0 \text{ for } S_n \leq 3Sm$$

$$= 1.0 + \frac{(1-n)}{n(m-1)} \left(\frac{S_n}{3Sm} - 1 \right)$$

for $3Sm < S_n < 3m Sm$

$$= 1/n \text{ for } S_n \geq 3m Sm$$

S_n = range of primary-plus-secondary stress intensity

m and n = material parameters

(3) The stresses produced by the equivalent linear portions of the radial thermal gradients are classified as secondary (Q in Table N-413) instead of peak (F in Table N-413). The equivalent linear portion of a radial gradient is defined as a linear radial gradient which develops the same thermal moment as the actual radial gradient.

(4) The rest of the fatigue evaluation stays the same as required in N.415 of Section III, except that the procedure of N-417.5 (b) need not be used.

The value of the material parameters m and n , are given for the various classes of code materials in the following table:

	m	n
Low alloy steel	2.0	0.2
Martensitic stainless steel	2.0	0.2
Carbon steel	3.0	0.2
Austenitic stainless steel	1.7	0.5
Nickel-Chrome-Iron	1.7	0.5

Meeting of October 31, 1969

Reprinted from MECHANICAL ENGINEERING March, 1970, a publication of The American Society of Mechanical Engineers.

Revisions* To (Effectively) ASME Boiler-Code Case 1441

NB-3228.3 Simplified Elastic-Plastic Analysis. The $3S_m$ limit on the range of primary-plus-secondary stress intensity (NB-3222.2) may be exceeded provided that

- (a) The range of primary-plus-secondary membrane plus bending stress intensity, excluding thermal bending stresses, shall be $\leq 3S_m$.
- (b) The value of S_a used for entering the design fatigue curve is multiplied by the factor, K_e , where

$$\begin{aligned}
 K_e &= 1.0 \text{ for } S_n \leq 3S_m \\
 &= 1.0 + \frac{(1-n)}{n(m-1)} \left(\frac{S_n}{3S_m} - 1 \right) \text{ for } 3S_m < S_n < 3m S_m \\
 &= 1/n \text{ for } S_n \geq 3m S_m
 \end{aligned}$$

S_n = range of primary-plus-secondary stress intensity

The values of the material parameters m and n are given for the various classes of Code materials in the following table:

	<u>m</u>	<u>n</u>	<u>T_{max} of</u>
Low alloy steel	2.0	0.2	700
Martensitic stainless steel	2.0	0.2	700
Carbon steel	3.0	0.2	700
Austenitic stainless steel	1.7	0.3	800
Nickel-Chrome-Iron	1.7	0.3	800

- (c) The rest of the fatigue evaluation stays the same as required in NB-3222.4, except that the procedure of NB-3227.6 need not be used.
- (d) The component meets the thermal ratcheting requirement of NB-3222.5.
- (e) The temperature does not exceed those listed in the above table for the various classes of Code materials.
- (f) The material shall have a minimum specified yield strength to minimum specified ultimate strength ratio of less than 0.80.

*Taken from the "Rewrite" of the ASME Boiler Code Section III, dated October, 1970.

With respect to this report, the significant changes in Case 1441 are

- (1) Elimination of the limit of 1,000 on cycles of stress range exceeding $3S_m$. Data given in this report indicates that such a limit is unnecessary.
- (2) Change in the n-value for austenitic stainless steel from 0.5 to 0.3. The formulas for K_e are

$$n = 0.5$$

$$1.0 + 1.43 [(S_n/3S_m)-1]$$

but not greater than 2.0

$$n = 0.3$$

$$1.0 + 3.33[(S_n/3S_m)-1]$$

but not greater than 3.33